RELATIONSHIP OF BODY AND SURFACE WAVE MAGNITUDES FOR SMALL EARTHQUAKES AND EXPLOSIONS

SEISMIC DATA LABORATORY REPORT NO. 245

AFTAC Project No.:	VELA T/2706
Project Title:	Seismic Data Laboratory
ARPA Order No.:	1714
ARPA Program Code No.:	2F-10
Name of Contractor:	TELEDYNE GEOTECH
Contract No.:	F33657-72-C-0009
Date of Contract:	01 July 1971
Amount of Contract:	$ 1,736,000
Contract Expiration Date:	31 October 1972
Project Manager:	Robert R. Blandford (703) 836-3882

P. O. Box 334, Alexandria, Virginia 22314

ABSTRACT

The relationship between body wave magnitude (m_b) and surface wave magnitude (M_s) is investigated using LRSM and VELA Observatory recordings of explosions at NTS, and small shallow earthquakes originating in Nevada, Alaska and central United States. Average M_s vs m_b curves based on data from many observing stations, as well as M_s vs m_b comparisons for individual stations are given. The estimates of m_b and M_s were corrected for stations at small epicentral distances using Evernden's and von Seggern's methods, respectively, in order not to bias the results when only close in or regional observations could be made.

Despite considerable scatter in individual M_s vs m_b determinations the results obtained for earthquakes show that on the average the relative excitation of P waves and Rayleigh waves is similar for the three source regions considered.

Least squares regression lines were fit separately to the observations of M_s vs m_b for NTS explosions and to those for small, shallow Nevada and Missouri earthquakes down to M_s = 2.6. The resulting slopes were very similar (1.04 ± .05 for explosions and 1.00 ± 0.10 for earthquakes) but the intercepts differed such that for given m_b the average M_s for NTS explosions is 0.62 to 0.65 smaller than for the earthquakes. For new events drawn from the same population the M_s vs m_b criterion can be expected to classify correctly 87.7% of NTS explosions and 72.8% of Nevada earthquakes for which any Rayleigh wave measurement can be made; however, several correctly discriminated events would fall sufficiently close to the best discriminant line that further analysis

of them would be needed before a convincing classification could be made. If one considers a restricted data set consisting of a swarm of southeast Nevada earthquakes in April 1966 and of contained NTS underground explosions, then for new events from the same population recorded at four or more stations with $3.6 \leq m_b \leq 5.04$ for explosions and $2.6 \leq m_b \leq 4.2$ for earthquakes, ($2.77 \leq M_s \leq 4.33$), it can be expected that 98.4% of the explosions and 99.0% of the earthquakes will be correctly classified. But again, in a practical sense no decision could be made for some additional percentage of events.

These data are from regional and close in stations, and it is not certain that the conclusions can be extrapolated for these low magnitudes to future teleseismic measurements made with new instruments and arrays. If a discriminant of this power is relied upon in a seismic region where there are several hundred earthquakes per year, then there will be several false alarms per year.

TABLE OF CONTENTS

LIST OF FIGURES

LIST OF FIGURES

LIST OF TABLES

INTRODUCTION

The purpose of this report is to define the relationship between body wave magnitude (m_b) and vertical Rayleigh wave magnitude (M_s) for small, shallow earthquakes and NTS explosions. In attempting to define this relationship, we faced several important difficulties.

(1) Reliable magnitude estimates for small events from conventional visual analysis of seismograms can be obtained only from the close stations. This in turn presents two additional difficulties: first, the distance correction for surface wave magnitudes differs from the standard Gutenberg correction applicable at teleseismic distances, and this correction must be established for each region; second, close-in P-wave magnitudes are difficult to obtain reliably because of the highly variable distance dependence of P-wave amplitudes.

(2) The smaller the event the fewer the stations observing the event and the smaller the signal-to-noise ratio at each station. Hence the magnitude errors are larger for the very small events. This is especially worrisome for earthquakes where significant radiation patterns can be anticipated.

We have attempted to circumvent these problems by using as nearly as possible a fixed array of receivers and a common source region for both earthquakes and explosions so that the influence of path and site location could be minimized or removed. Stations covering a large range of azimuths were used whenever possible, to compensate for radiation pattern effects.

Finally, reasonably large samples of earthquakes and explosions spanning the P-wave magnitude range of 2.5 to 6.0 were analyzed to obtain statistical control on the relation between body and surface wave magnitudes for the smaller events.

PROCEDURE AND DATA USED

Evaluating the relationship between M_s and m_b for small events necessitates measurements at small distances over continental paths. In this study for the explosion data we used shot reports from 48 Nevada Test Site explosions (Table I) recorded at LRSM and VELA station networks. Since we are assured of a common source region, we can look at P and Rayleigh wave amplitudes at each station, thereby effectively eliminating distance and site response factors in determining the relationship between these two phases as a function of magnitude. Also there is theoretical evidence to support the hypothesis that source spectra for explosions are similar over a broad range of magnitudes (von Seggern and Lambert. 1969). Therefore we expect some systematic relationship between M_s and m_b to be present for explosions.

Assuming dissimilar source spectra for earthquakes, we selected many events from a source region sufficiently large in area to include many possible source mechanisms, and yet small enough that distance effects are relatively minor. In this manner the mean ratio of P to Rayleigh wave amplitude can be defined for earthquakes. The group of Nevada earthquakes selected for analysis ranged in NOS P-wave magnitude from 3.6 (or no estimate at all) to 5.2; however, as well be seen later, the larger magnitudes appear to be overestimated. In addition, recordings of 133 aftershocks from the Great Alaskan earthquake of 1964 were analyzed on KN-UT and RK-ON records to determine the empirical relationship between P and Rayleigh waves transversing longer continental paths. To determine whether there are strong regional differences in relative excitation of P and Rayleigh waves for the areas studied we

also compared the M_s/m_b relationship for 18 Nevada and two Missouri earthquakes (Table II) to that obtained from the Alaska source region.

METHOD OF MAGNITUDE CALCULATIONS

Gutenberg and Richter's (1956) definition of body wave magnitude is accepted by practically all seismological organizations as the standard; however, Evernden (1967) showed that for distances less than 20° it is necessary to adjust the distance correction factor to obtain magnitudes consistent with teleseismic body wave magnitudes. He obtained the empirical corrections applicable for the Western United States and we have used his formulae for the determinations of m_b at the nearer stations. In this paper we refer to adjusted body wave magnitudes (m_b) which combine teleseismic estimates with values obtained at distances less than 20° using Evernden's distance corrections.

It should be noted that the corrections for small epicentral distances depend strongly on the crust and upper mantle structure which is known to vary substantially from region to region, so the distance correction factors must be determined separately for each source region of interest.

Calculation of the surface wave magnitude for events at distances greater than 15° is based on Gutenberg's (1945) formula:

$$M_s = \log A_H + 1.656 \log\Delta + 1.818 + C + D$$

where A_H = 0.5 peak-to-peak amplitude in microns at T = 20 seconds for the horizontal radial component of Rayleigh wave; $1.656 \log\Delta$ is the distance correction factor; Δ is measured in degrees. This correction is limited to the distance range 15° to 130°; C is the site correction factor; D is the correction

for depth of source, azimuth, etc. For this study we assume that C and D are zero, and use the following relation adopted by Geotech (1964):

$$M_s = \log (A_z/T) + 1.66 \log\Delta - 0.18$$

where A_z is the peak-to-peak amplitude in millimicrons, and T is the corresponding period in seconds for the vertical component of Rayleigh wave; Δ is the distance in degrees. These two formulas are identical at T = 20 seconds. The Geotech formula does not consider ellipticity (A_H/A_Z); however, for periods in the range 15 to 17 seconds and an ellipticity of 0.8, the variation of M_s (Geotech) and M_s (Gutenberg) is only ±0.03 magnitude units. Since small magnitude events observed over continental paths have their maximum measurable amplitudes in this range of periods, the Geotech formula is compatible with Gutenberg's.

It is important to note that this formula gives a magnitude 0.18 less than the NOS and Basham (1969) estimates. Their formulas are:

$$\text{NOS: } M_s = \log (A/T) + 1.66 \log\Delta + 3.3$$

where Δ is the distance in degrees and A/T = amplitude, zero to peak in microns/sec;

$$\text{Basham: } M_s = \log (A/T) + 1.66 \log\Delta + 0.3$$

where Δ is the distance in degrees and A/T is the zero-to-peak amplitude in millimicrons/sec.

For distances less than 15° we use a modified distance correction factor for surface waves (von Seggern, 1970) derived from Rayleigh wave amplitude measurements of 30 Nevada Test Site explosions having four or more Rayleigh wave amplitude measurements at distances greater than 15°. *The resulting data include 341 values of M_s at distances less than 15° and 240 values at distances greater than 15°. *von Seggern has tested statistically the hypothesis that a single straight line of the form $M_s = \log\Delta + C$, determined by least squares analysis would fit both populations better than would two lines. This hypothesis is rejected at the 99.95% confidence level. A least squares fit to the data from less than 15° distance, normalized to a magnitude determined from data at distances greater than 15°, provides a modified magnitude (M_s^c) for distances less than 15°

$$M_s^c = \log (A/T) + 1.16 \log\Delta + 0.74.$$

Although it is an approximation this expression gives magnitudes consistent with teleseismic values. Therefore, the vertical Rayleigh wave magnitude used in this paper is termed "Adjusted M_s" which is the average of all M_s^c and M_s for a given event.

*In Figure 1 these magnitudes are plotted as a function of distance after the magnitude determined from measurements at distances greater than 15° have been subtracted.

RESULTS AND DISCUSSION

Figure 2 shows the relationship of body wave magnitudes to Rayleigh wave magnitudes at KN-UT for 37 explosions at an average distance of 2.55°. All the raw data were taken from shot reports. A least squares linear fit to the log of the respective amplitudes (in the form of body and surface wave magnitudes) gives:

$$M^{c}_{SKN} = (1.03 \pm 0.09)\, m_{KN} - (1.13 \pm 0.49).$$

Figure 3 shows the same picture at HN-ME for 19 explosions at an average distance of 36.6° with the following results:

$$M^{c}_{SHN} = (0.97 \pm 0.14)\, m_{HN} - (0.62 \pm 0.78).$$

The errors given for the slopes and intercepts throughout this paper are 95% confidence limits. Basically then, these results show that at a given distance the surface wave magnitude is directly proportional to the body wave magnitude for both near-in and teleseismic distances, even though the surface waves decay differently with distance in the two distance ranges. These distance correction factors should be applied to both body and surface wave magnitude estimates in order to obtain an unbiased M_s vs m_b comparison of earthquakes and explosions of different sizes in different regions.

Figure 4 shows average adjusted M_s vs m_b data for 47 Nevada Test Site explosions and a chemical explosion

at Climax, Colorado. We shall return to this figure later to discuss discrimination. Here we wish to concentrate on the calculated slopes for explosions. The least squares fit to these data uses 38 of 48 explosions. Nine explosions are excluded which have three or less stations with surface wave amplitude measurements. We also discarded PAR from the analysis because of its obvious anomalously low position. The least squares fit to these 38 explosions gives:

$$\text{Adjusted } M_s = (1.04 \pm 0.05)\, m_b - (0.74 \pm 0.24).$$

The m_b range for the above results is 3.59 to 6.25 and the variance of the fit may be attributed to factors such as the partially variable network of LRSM recording stations from event to event, the different geologic media in which the explosions took place, and errors in m_b and/or M_s estimates themselves. Further, there is evidence that at higher magnitudes ($m_b > 5.8$) the source spectra may change sufficiently to perturb the linearity of the M_s/m_b slope (von Seggern and Lambert, 1969). With regard to the seven explosions having three or less stations receiving the long-period signal, we would expect that these would be biased toward higher apparent surface wave amplitudes and cause a large estimate of M_s relative to m_b. Six of the seven lie above the least-squares line, and only one is below it (Figure 4).

On the other hand both the M_s and the m_b for small earthquakes are biased toward higher values since there are only a few stations with observable P waves in the cases where there are only 2 or 3 surface wave measurements. That is, we are using only the larger amplitude P and Rayleigh waves so the bias is diagonally upward along the $M_s - m_b$ curve. Thus even though the scatter increases there is no apparent tendancy

for the earthquake M_s - m_b relationship to change its slope as there is for the explosions. The result is to decrease the mean discrimination capability. This can be seen in Figure 4.

This is further verified for explosions and earthquakes when comparisons are made of recordings at common stations for a large companion event. As a first step in the comparison we determine an M_s^T for these events and their companion events. M_s^T is based on body-wave magnitude (i.e., $M_s^T = 1.04\ m_b - 0.74$ for explosions and $M_s^T = 1.00\ m_b + 0.06$ for earthquakes). Further, we determine for the larger companion event an $\overline{M}_s$ using the same three or less stations that recorded the small event. Computing $\overline{M}_s - M_s^T$ for both sets of events, Table V, we find that five of the seven explosions with three or less Rayleigh readings do have larger Rayleigh-wave magnitudes relative to the companion event; Stutz is the exception, and Pampas does not have an event for comparison. The analysis for earthquakes yields a similar answer. All but two $\overline{M}_s - M_s^T$ for the seven small earthquakes are greater than $\overline{M}_s - M_s^T$ for the larger companion event. When $\overline{M}_s - M_s^T$ for the small events are plotted as a function of $\overline{M}_s - M_s^T$ for the companion events, no correlation is observed. Thus, our results are compatible with the hypothesis that "random" effects or source differences cause large amplitudes to be observed at certain stations. The results are not compatible with the hypothesis that static station effects cause large amplitudes at these stations.

Included in Figure 4 are the mean error bars of M_s and m_b for explosions in the m_b ranges of 3.50 to 4.50, 4.51 to 5.50, and 5.51 to 6.60; and for earthquakes in the m_b ranges of 2.00 to 3.50, 3.51 to 5.0, and 5.01 to 5.65. The size of the error bars reflect the standard deviation of the mean (i.e.,

$\hat{\sigma m} = \sigma/\sqrt{n} = \left(\sum_{i=1}^{n} \left[\frac{(M_i - \bar{M})^2}{n(n-1)} \right] \right)^{1/2}$. Clearly, the error in magnitude determinations for earthquakes increases with decreasing size. This is not the case for explosions. The large explosions show increasing error partially due to the fewer number of stations used in the magnitude determinations for Benham and partly due to large standard deviations of individual station estimates.

The importance of the distance correction factor for $\Delta < 15°$ is again emphasized in Figure 5. In this figure, we show M_s (Geotech) vs m_b in which the correction factor 1.66 log Δ was applied for all distances. The least squares fit to the same 38 explosions discussed above is

$$M_s = (1.21 \pm 0.06)\ m_b - (1.89 \pm 0.28).$$

Basham (1969) obtained similar results ($M^P = 1.24\ m_b - 1.76$) for 26 Nevada explosions recorded by the Canadian station network. The difference in intercepts (1.89 - 1.76 = 0.13) is largely due to the difference in the M_s formulation (0.18) between Basham and Geotech (Magnitude Section).

Figure 6 shows the source regions for the aftershocks from the Great Alaska earthquake, the Nevada earthquakes and the Missouri earthquakes. The figure also shows the locations of the stations used.

Figures 7 and 8 show the P wave and Rayleigh wave magnitudes observed at RK-ON and KN-UT from the Alaska source region. A least squares fit to these data gives the following results:

For RK-ON:

$$M_{sRK} = (1.01 \pm 0.16)\, m_{RK} - (0.05 \pm 0.74),$$

$$\text{for } 3.9 \leq m_{RK} \leq 5.9,$$

For KN-UT:

$$M_{sKN} = (0.97 \pm 0.18)\, m_{KN} + (0.11 \pm 0.83),$$

$$\text{for } 3.8 \leq m_{KN} \leq 5.6.$$

Even though there is much scatter in both plots, the mean slopes are remarkably similar.

Pomeroy (1967) shows a plot of log peak-to-peak Rayleigh wave amplitudes in millimeters (uncorrected for instrument response) versus NOS body wave magnitudes (m_b = 3.6 to 5.3) for 127 aftershocks from the Great Alaska earthquake recorded at College, Alaska. Figure 9 shows a least squares fit to these data giving:

$$\log A(\mu m) = (1.01 \pm 0.08)\, m_{NOS} - (3.42 \pm 0.34).$$

The epicentral distance varies for these events from 315 to 1045 km. However, by using a mean distance of 680 km (6.1°) and the indicated instrumental gain of 1500 we can estimate approximately the intercept values in terms of M_s and M_s^c:

$$M_{sCOL} = 1.01\, m_{NOS} - (\approx 0.78)$$

and the

$$M^c_{sCOL} = 1.01\, m_{NOS} - (\approx 0.26).$$

In spite of the obvious scatter in Figure 9, the slope of 1.01 is essentially the same as the slopes determined at RK-ON

and KN-UT. The actual value of the intercept depends on the proper distance, distance correction factors and site corrections for both body wave and Rayleigh wave amplitudes; however, the approximate intercept shown for M^c_{sCOL} is comparable to those obtained for RK-ON and KN-UT. The least squares fits to the above data are summarized in Figure 10.

Thus, as for the Nevada Test Site explosions and Nevada earthquakes, these Alaskan earthquakes ($3.6 \leq m_b \leq 5.9$) observed at fixed distances give Rayleigh wave magnitudes directly proportional to body wave magnitudes, but with considerably greater scatter about the mean line. With the appropriate distance corrections they may also show similar intercepts for the M_s vs m_b curve.

Because of differing earthquake source mechanisms in any specific source region, good azimuthal coverage of stations is necessary to determine mean surface wave and body wave magnitudes reliably. For the Nevada and Missouri source regions we have sufficient azimuthal coverage only at small distances (Figure 6). In Figure 4, a least squares fit to the Nevada and Missouri earthquakes combined, omitting events for which M_s was determined at three stations or less show:

$$\text{Adjusted } M_s = (1.00 \pm 0.10)\, m_b + (0.06 \pm 0.32)$$

in the magnitude range $2.6 \leq m_b \leq 4.2$. These results are consistent with those discussed earlier, which were obtained from the Alaska source region at COL, RK-ON, and KN-UT, Figure 10. Included in Figure 4 are twelve additional Western United States earthquakes ($4.7 \leq m_b \leq 5.7$) listed by Basham, 1969. The events were recorded by ten or more Canadian stations and therefore the effect on the mean magnitude due to including the three stations at distances less than 15° is smaller than for the

cases where only a few teleseismic observations were used. Further, we do not correct M_s for the 0.18 difference in surface wave formulations discussed previously. Thus, the separation between the explosions and Bashams earthquakes is enhanced somewhat.

We have also added to Figure 4 and listed in Table IV M_s/m_b for four earthquakes: two from Utah, one from Colorado, and one from New Mexico, as well as two explosions, one from Colorado and one from New Mexico. These data points closely conform to those derived for the NTS events.

From these data it appears that a linear relationship exists, with slope $\simeq$ 1.0, between M_s and m_b for earthquakes from m_b = 2.6 to 4.9 and for explosions from m_b = 3.6 to 5.4. These results suggest that on the average both the explosion and earthquake populations in Nevada approach the same linear dependence and slope of M_s vs m_b at small magnitudes but with different intercepts, so that the population means are different at each given magnitude in the range cited above. By constraining the slopes of Adjusted M_s vs m_b for both earthquakes and explosions to be equal, the surface wave magnitude separation is 0.62, compared to 0.65 found by Basham from mostly teleseismic observations. For the still smaller events, low signal-to-noise ratios and fewer total observations cause all the magnitude estimates to be suspect, so we can draw no conclusion concerning their M_s vs m_b behavior.

Single station M_s vs m_b observations

The question naturally arises whether the composite M_s/m_b data presented above is biased so that the event populations do not separate to the degree suggested by the statistical analysis. Low signal-to-noise ratios, source spectral para-

meters or radiation patterns, and the limited station network can certainly introduce some bias. But the fact that Basham obtained a separation of 0.65 magnitude units from mostly teleseismic measurements and a completely different station network, compared to our difference of 0.62 magnitude units (Figure 10), suggests that the separation is real. Furthermore, if differences in M_s vs m_b persist at single stations, then regardless of any bias, the M_s/m_b criterion for identification remains valid.

In this section we consider body-wave and Rayleigh-wave amplitudes at MN-NV, KN-UT, and UBO for explosions and earthquakes. In the previous section all explosion data were taken from shot reports. In this section all explosions were reanalyzed and care was taken to measure (whenever possible) the same phase or cycle of P and Rayleigh waves for both explosions and earthquakes. Figures 11 and 12 show seismic signals of earthquakes and explosions recorded on the short-period and long-period vertical instruments at MN-NV. Figure 13 shows the short-period signals at higher gains; measurements of the same cycle of the P-wave is possible for the explosions, but only for the initial portion of the signal. It is clear that this is not usually the case for the earthquakes. However, the same cycle of Rayleigh waves can be measured for both types of events. Therefore we expect that much of the scatter in the data will be due to inconsistencies of the P-wave amplitude measurements. This factor will be discussed in more detail later.

All earthquakes were selected from the Preliminary Determinations of Epicenters (NOS) event listing from January 1963 to January 1970. Fifty-four earthquakes were analyzed which occurred around MN-NV, and thirty around KN-UT, between

distances of 200 to 300 km. This distance range corresponds to the distances between Nevada explosions and the same stations. When the same distance criterion was attempted at UBO, most of the earthquakes listed were not large enough to be recorded. Accordingly at UBO the distance range was set from 200 to 500 km. Fifty-six earthquakes were analyzed around UBO, and the amplitudes corrected for distance by use of the body-wave and surface-wave magnitude formulas discussed earlier. The event locations relative to the stations and NTS are shown in Figure 14 and listed in Table III. No attempt was made to include events common to all stations, since we need only to fit the criteria of having the events in the indicated distance ranges and a large sample of events over the magnitude range of 2.8 to 5.2 (NOS).

P-wave and Rayleigh wave amplitudes listed in Table III are shown in Figures 15 and 16 for MN-NV, KN-UT and magnitudes for UBO in Figure 17. Although there is little overlap in the data there is clear separation between the least-square lines for MN-NV and KN-UT. Of the 30 events recorded at KN-UT, five had no visible Rayleigh waves; of the 54 events recorded at MN-NV, four had no visible Rayleigh-waves; and of the 56 events recorded at UBO, 17 had no visible Rayleigh waves. In the least squares determination of M_s vs m_b for KN-UT and MN-NV no observations were included in the m_b magnitude range where some events had no visible Rayleigh waves; this limit is shown by the vertical dashed line in Figures 15 and 16. We did not determine least squares lines for the populations at UBO because of the obvious lack of earthquakes with P magnitudes equivalent to those of the explosions.

Note that these data are for the NTS region, and therefore, for a slope of 1.0 it would be required to use Evernden's (1967) corrections. When these are not used, the expected slope is approximately 1.2. Also, the regression lines are poorly determined, in particular we feel that a slope of 1.2 is within reasonable confidence limits for all of the lines in Figures 15 and 16.

There is apparent separation between populations at single stations for the small magnitude events, but because of the overlap and scatter of data points it is clear the M_s/m_b at one close in station alone is not adequate in practice for identification, unless some other measurement techniques such as spectral amplitudes can reduce the variance.

As stated previously, the usual problems associated with amplitude measurements are involved here: low signal-to-noise ratio, radiation pattern, and depth of source. Site and path effects are minimal for the explosions observed at single stations; however these effects for the earthquakes studied obviously perturb both P and Rayleigh amplitude measurements to a greater degree because of the larger spatial distribution of epicenters (Figure 11).

The deviation at a single station due to variation in either the Pn or Rayleigh measurement can be demonstrated by plotting on one axis the amplitude for a given event predicted from its teleseismic magnitude using Evernden's (1967) or von Seggerns (1970) formulas as appropriate. Figures 18 and 19 show measured Pn amplitudes versus predicted Pn amplitudes at KN-UT and MN-NV for 25 explosions. Figures 20 and 21 show Rayleigh-wave amplitudes versus predicted Rayleigh-wave amplitudes for the same stations. A least squares fit to these data

give:

[Figure 18, KN-UT]:

$\log A/T\ (Pn) = -0.039 + 1.15 \log A/T\ (\text{Predicted } Pn)$
and $\sigma = 0.32$

[Figure 19, MN-NV]:

$\log A/T\ (Pn) = -0.107 + 1.16 \log A/T\ (\text{Predicted } Pn)$
and $\sigma = 0.36$

[Figure 20, KN-UT]:

$\log A/T\ (LR) = 0.044 + 0.975 \log A/T\ (\text{Predicted } LR)$
and $\sigma = 0.20$

[Figure 21, MN-NV]:

$\log A/T\ (LR) = 0.326 + 1.100 \log A/T\ (\text{Predicted } LR)$
and $\sigma = 0.26$.

These comparisons of observed versus predicted amplitudes show that there is less scatter for the Rayleigh-wave amplitudes than for the Pn amplitudes at both stations. We carry this comparison further and show measured Rayleigh amplitudes versus predicted Pn amplitudes, and vice versa.

Note that if there is scatter for the abscissa data, then slopes calculated by least squares may be too small because the extreme points may be displaced laterally. In a particular case there is no scatter then the slopes will be greater than usually seen. This may explain the bias toward slopes greater than 1.0 in Figures 18 through 21. The bias toward an incorrect slope will be greater for small data samples than for larger ones.

Figures 22 and 23 show measured Rayleigh amplitudes

versus predicted Pn amplitudes at KN-UT and MN-NV. Figures 25 and 26 show predicted Rayleigh amplitudes versus actual Pn amplitudes. A least squares fit to these data gives:

[Figure 22, KN-UT]:

Log A/T(LR) = 0.160 + 1.178 log A/T (Pn Predicted)
and σ = 0.18,

[Figure 23, MN-NV]:

log A/T(LR) = -0.436 + 1.330 log A/T (Pn Predicted)
and σ = 0.30,

[Figure 24, KN-UT]:

log A/T(LR Predicted) = 0.799 + 0.810 log A/T (Pn)
and σ = 0.32,

[Figure 25, MN-NV]:

log A/T(LR Predicted) = 0.789 + 0.770 log A/T (Pn)
and σ = 0.34.

Thus, at both stations where the Pn amplitudes are based upon teleseismic magnitudes, the standard deviation is less than that obtained using the predicted Rayleigh amplitudes. Also, the slopes are greater or less than 1.0 in accordance with the argument above. At KN-UT a large portion of the scatter is due to the Pn amplitudes, whereas for MN-NV the scatter seems to be about equally attributable to both Pn and Rayleigh amplitude measurements. It is important to note also that the mean of the slopes in Figures 22 and 24 for KN-UT is 0.994 ([1.178 + 0.810]/2 = 0.994) and in Figures 23 and 25 for MN-NV is 1.008 ([1.330 + 0.770]/2 = 1.050). This suggests that the predicted M_s is directly proportional to predicted m_b, and of course one expects this because Figure 4 shows a slope of 1.04 for explosions.

We now return to Figure 4 to finally determine the expected discrimination power of the average M_s-m_b discriminant. We use the linear discriminant function with equal a-priori probability, discussed recently by Shumway and Blandford (1970). We first restrict the data set and apply the analysis to the data in Figure 4 from Nevada earthquakes and explosions alone. This excludes the events in Missouri, Colorado, New Mexico and Utah; and all except two of Basham's earthquakes. We also exclude Sedan (a cratering shot), and Small Boy (an air shot). Then from the resulting sample of 20 earthquakes two were misclassified; and from the sample of 45 explosions five were misclassified. Applying the technique described by Shumway and Blandford (1970), for prediction of performance on new data we obtain expected misclassification rates of 12.3% for the Nevada explosions, and 27.2% for the Nevada earthquakes. In Figure 4 we have shown the best discrimination line for this determination. These results are the worst we can expect from these data since events having magnitude determinations with three or less stations are included in the analysis.

Further, excluding all events having three or less station magnitude determinations we arrive at the data set in Figure 26. One earthquake and one explosion are misclassified. The expected misclassification rates on new data are 1.6% for explosions and 0.9% for earthquakes.

In addition, it is reasonable to constrain these Nevada data to a lower limit of $M_s = 2.77$ since this is slightly above the point at which some Rayleigh waves are not detected for Nevada earthquakes. The upper limit is set at $M_s = 4.33$ which conforms to the Nevada earthquake data analyzed for

this report and excludes the two earthquakes from Basham's data. As before we exclude all events with magnitudes determined from three or less stations and SMALL BOY and SEDAN. Using these Nevada events in the magnitude range $2.77 \leq M_s \leq 4.33$, (i.e. $2.6 \leq m_b \leq 4.2$ earthquakes; $3.6 \leq m_b \leq 5.04$ explosions) we misclassify no earthquakes and no explosions; however, the estimated misclassification rates on new data are 1.6% for explosions and 1.0% for earthquakes. Inclusion of the New Mexico and Colorado explosions, and Colorado, New Mexico, Missouri and Utah earthquakes does not change any of the above expected misclassification rates.

It should be emphasized however that all of the Nevada earthquake data is from a swarm of events in Southeast Nevada, approximately 10 by 10 km in area, and this data is the bulk of the total even when the events from other states are included. And of course the NTS region, though varied in its geology, has a small area.

CONCLUSIONS

1. For earthquakes in the magnitude range $2.6 \leq m_b \leq 5.6$, the relative excitation of Rayleigh waves and P waves as indicated by the M_s and m_b observations, appears on the average to be similar for three different source regions. That is, both the slope and intercept of the fitted M_s vs m_b curves are the same, to within the error limits. However, we do not infer that this holds for every source region.

2. Based on the least squares regression lines, Nevada Test Site explosions of a given m_b on the average give surface wave magnitudes about 0.62 to 0.65 smaller than corresponding P wave magnitude earthquakes in Nevada and Missouri, down to magnitudes (m_b) of 3.6. Although there is greater scatter in observations for still smaller earthquakes the trend of M_s vs m_b does not appear to change in this range ($2.6 \leq m_b \leq 3.6$).

3. The lower magnitude limits for explosions and earthquakes are dependent upon the detectability of the Rayleigh waves and scatter of the P and Rayleigh wave data due to factors such as problems of radiation patterns, regional variations, small S/N and small number of stations.

4. On the basis of the observations presented here and linear discriminant analysis of the averages, the M_s vs m_b criterion can be expected to correctly classify 87.7% of NTS explosions and 72.8% of southeast Nevada earthquakes for which any Rayleigh wave measurement can be made.

Further, constraining the magnitude range to $M_s \geq 2.77$, (this constrains the earthquake $m_b > 2.60$, and the explosion

m_b > 3.60), requiring Rayleigh wave measurements at four or more stations, and applying the linear discriminant analysis, the M_s vs m_b criterion can be expected to correctly classify 98.4% of explosions and 99.0% of southeast Nevada earthquakes. Inclusion of the New Mexico and Colorado explosions, Colorado, New Mexico, Missouri and Utah earthquakes to the Nevada data does not change the classification percentages indicated above. However, the above results are based on the ability to make reliable estimates of small event magnitudes. Reliable estimates are highly dependent upon having numerous seismometers at regional or short epicentral distances, high S/N ratios, ≈ 180° azimuthal control, and proper corrections for regional propagation path effects. Furthermore the bulk of the earthquake data comes from a single swarm of southeast Nevada events.

The problem of detecting Rayleigh waves from small magnitude events at teleseismic distances still exists. There is, furthermore no direct evidence that, for small magnitudes, the discrimination power of teleseismic measurements is equal to that of regional measurements.

REFERENCES

Analyst's Handbook, 1964, Report No. 64-51, Geotechnical Corp., Garland, Texas , 20 May.

Basham, P.W., 1969, Canadian magnitudes of earthquakes and nuclear explosions in south western North America: Geophys. J.R. Astr. Soc., v. 17, 1.

Evernden, J.F., 1967, Magnitude determination at regional and near-regional distances in the United States: Bull. Seismol. Soc. Am., v. 57, p. 591.

Gutenberg, B., 1945, Amplitudes of surface waves and magnitudes of shallow earthquakes: Bull. Seismol. Soc. Am., v. 35, p. 3.

Gutenberg, B. and Richter, C.F., 1956, Magnitude and energy of earthquakes, Annali. Geofis., v. 9, p. 1.

Pomeroy, P., 1967, The distance ranges and minimum magnitudes required for detection of surface waves, Institute of Science and Technology, The University of Michigan, Report No. 7885-1-X, v. 53.

Shumway, R.H. and Blandford, R.R., 1970, A simulation of seismic discriminant analysis: Seismic Data Laboratory Report No. 261, Teledyne Geotech, Alexandria, Virginia.

von Seggern, D.H., 1970, Surface-wave amplitude-versus-distance relation in the Western United States, Seismic Data Laboratory Report No. 249, Teledyne Geotech, Alexandria, Va.

von Seggern, D.H. and Lambert, D.G., 1969, Dependence of theoretical and observed Raylcigh-wave spectra on distance, magnitude and source type: Seismic Data Laboratory Report No. 240, Teledyne Geotech, Alexandria, Va.

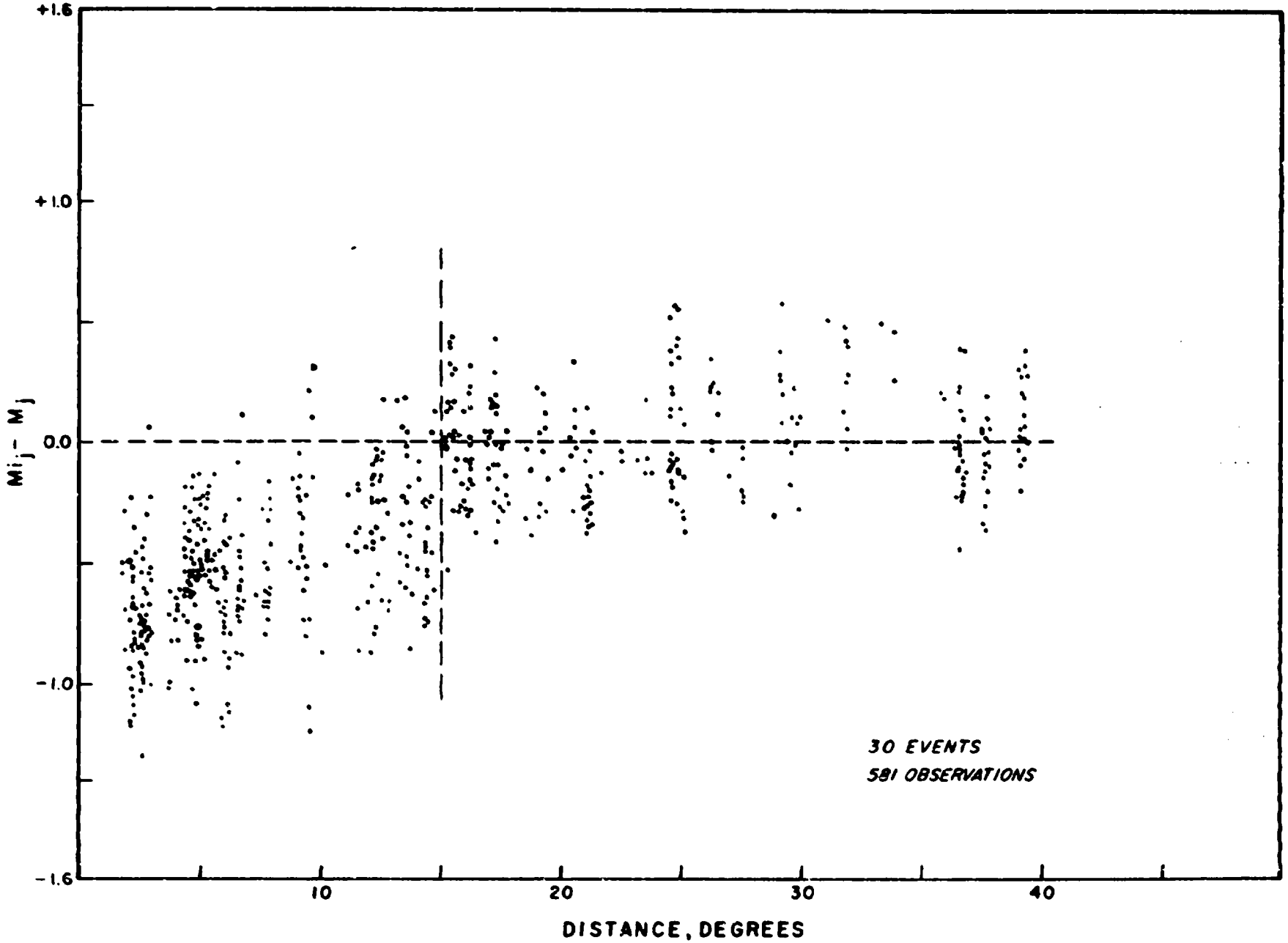

Figure 1. von Seggern's individual magnitude deviations for NTS explosions.

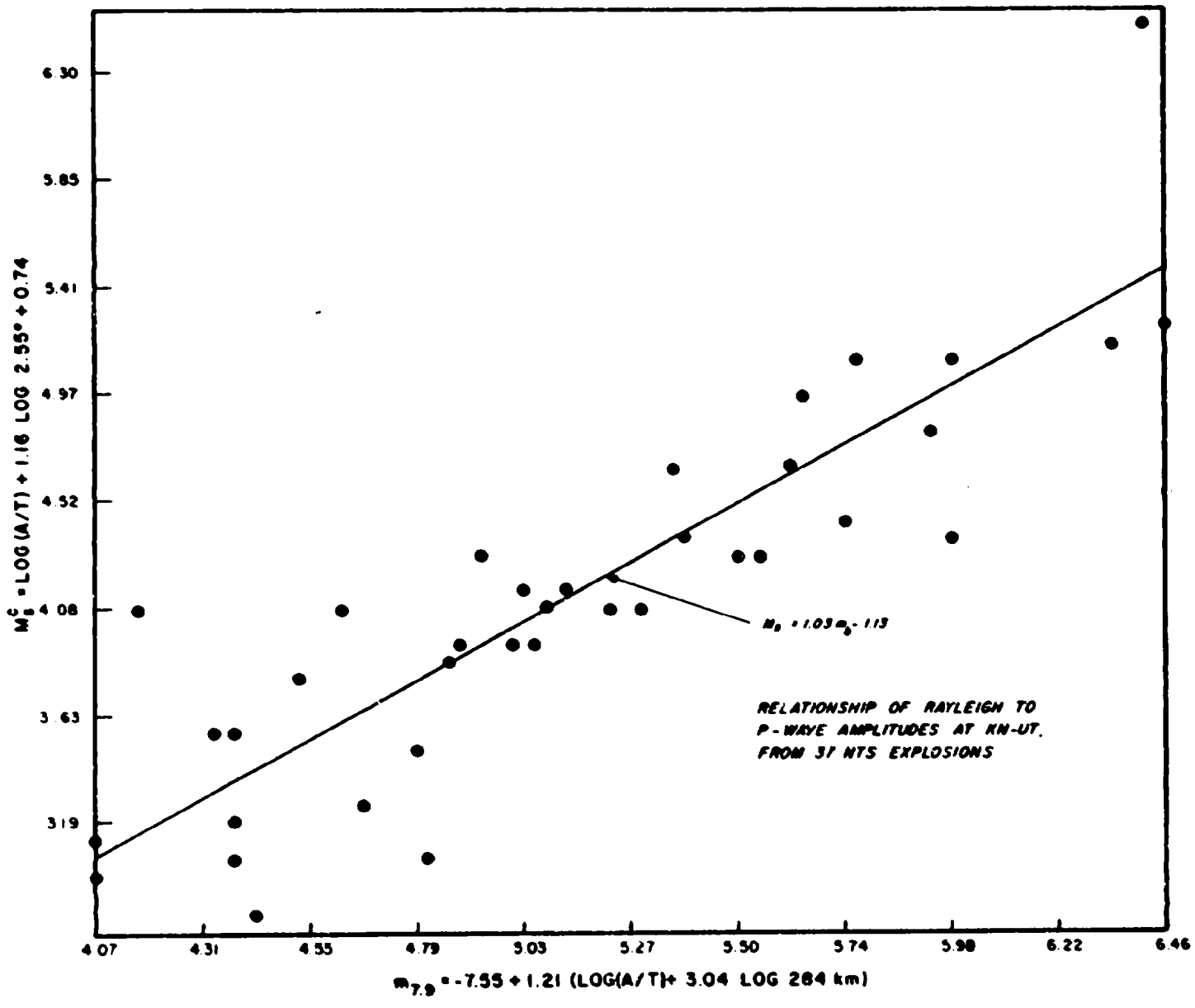

Figure 2. Relationship of Rayleigh wave amplitude to P-wave amplitudes at KN-UT from 37 NTS explosions.

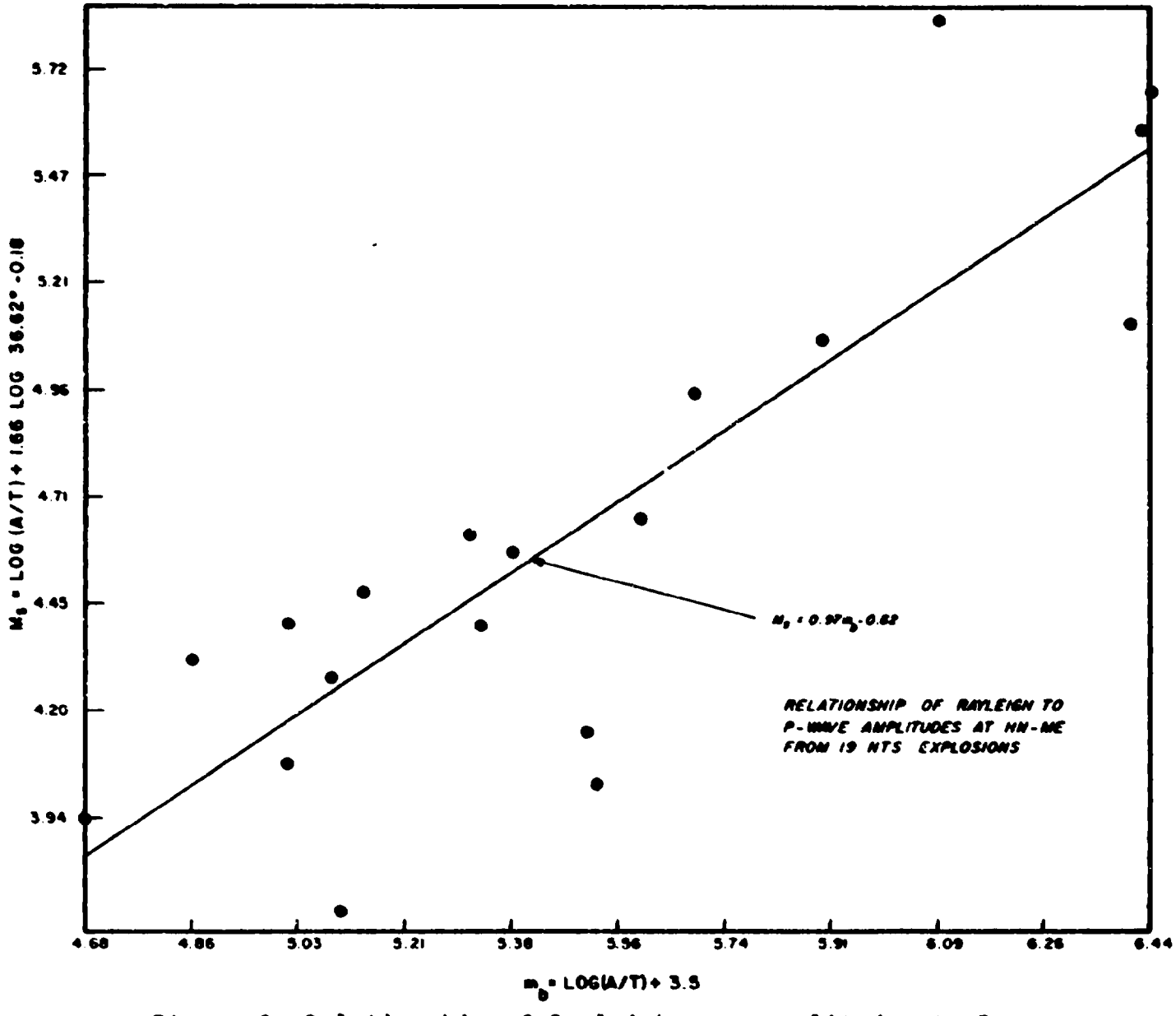

Figure 3. Relationship of Rayleigh wave amplitudes to P-wave amplitudes at HN-ME from 19 NTS explosions.

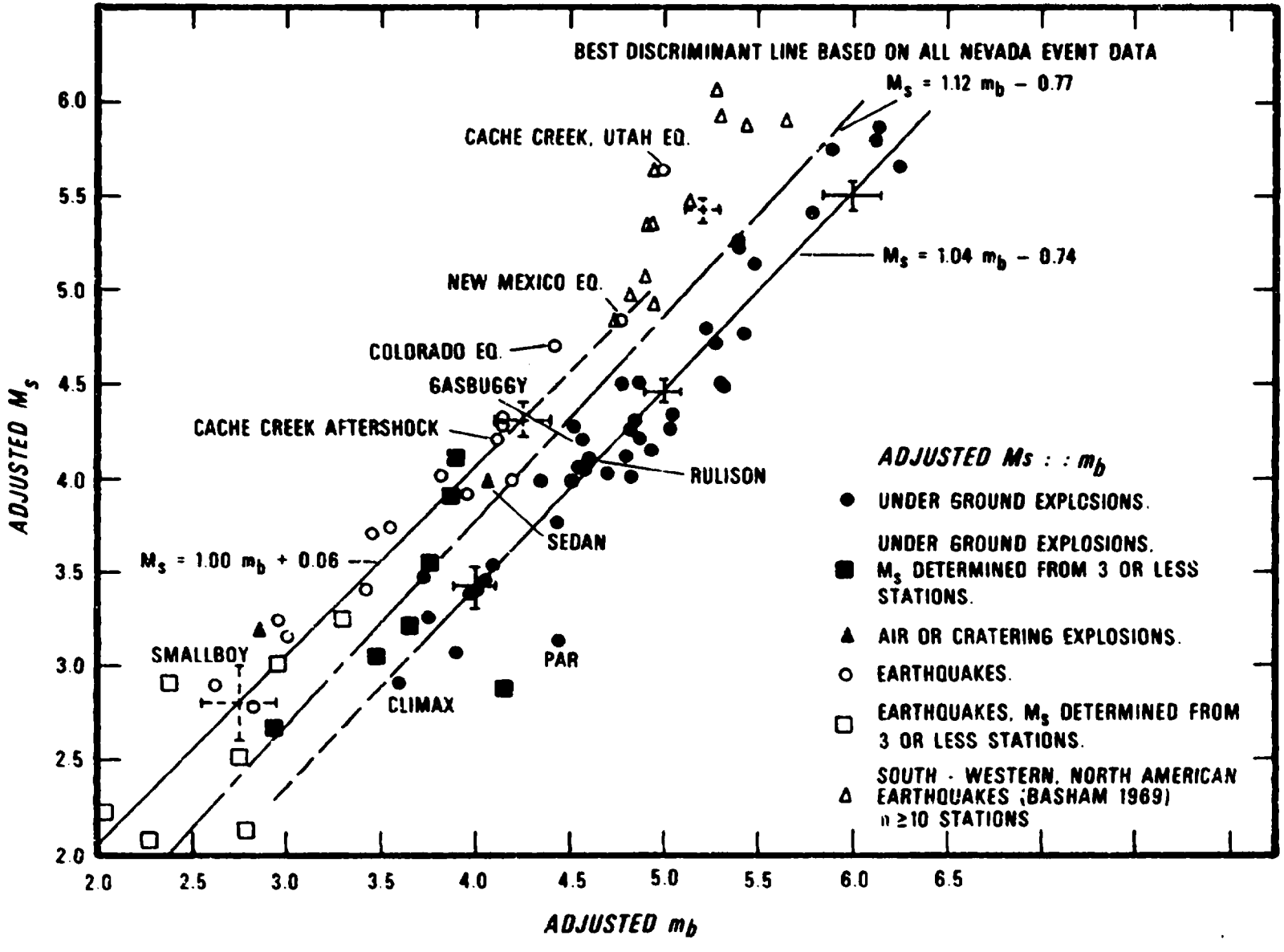

Figure 4. Adjusted M_s versus m_b for western United States explosions, earthquakes and Missouri earthquakes.

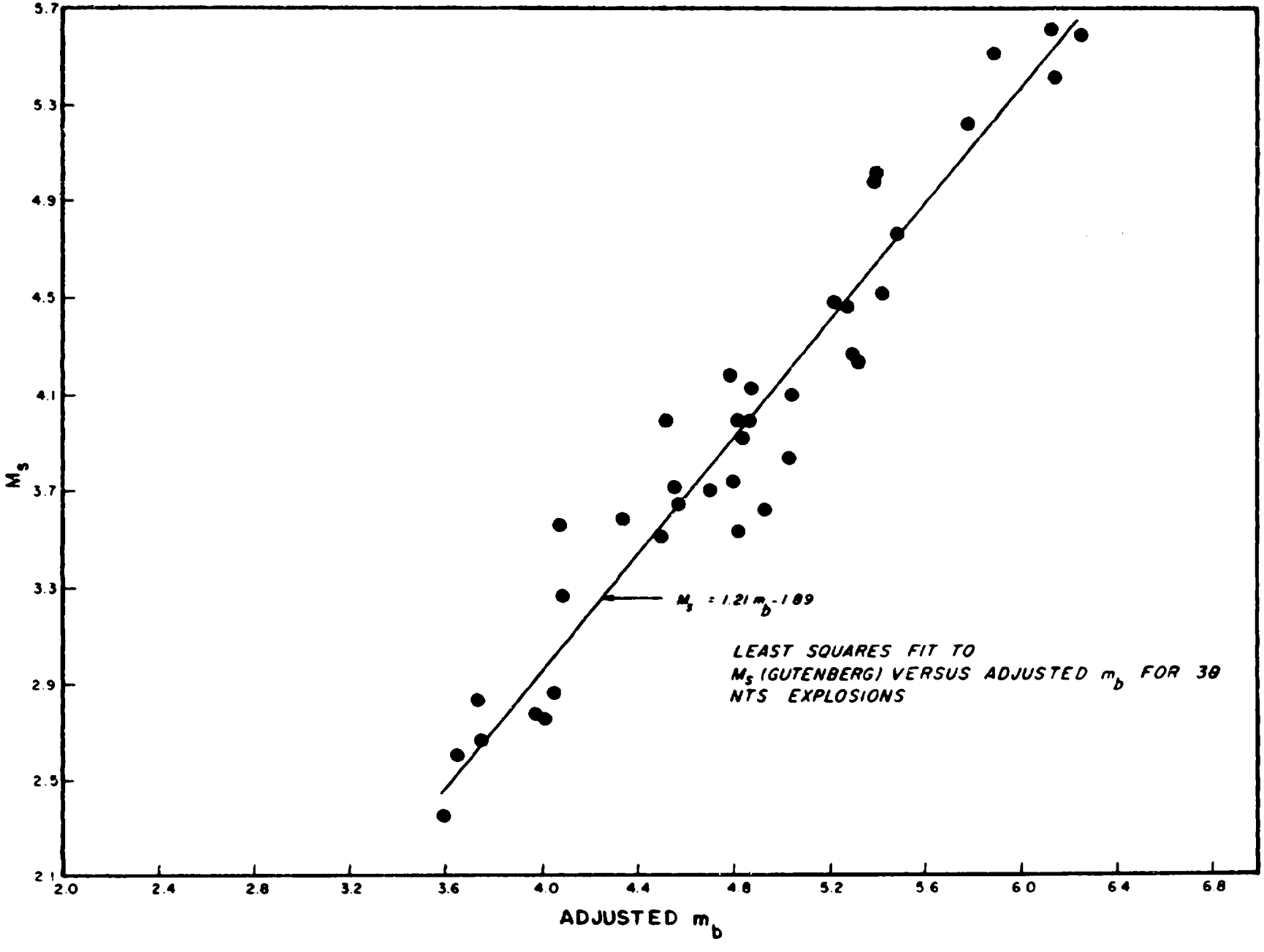

Figure 5. Least squares fit to M_S (Gutenberg) versus m_b for 39 NTS explosions.

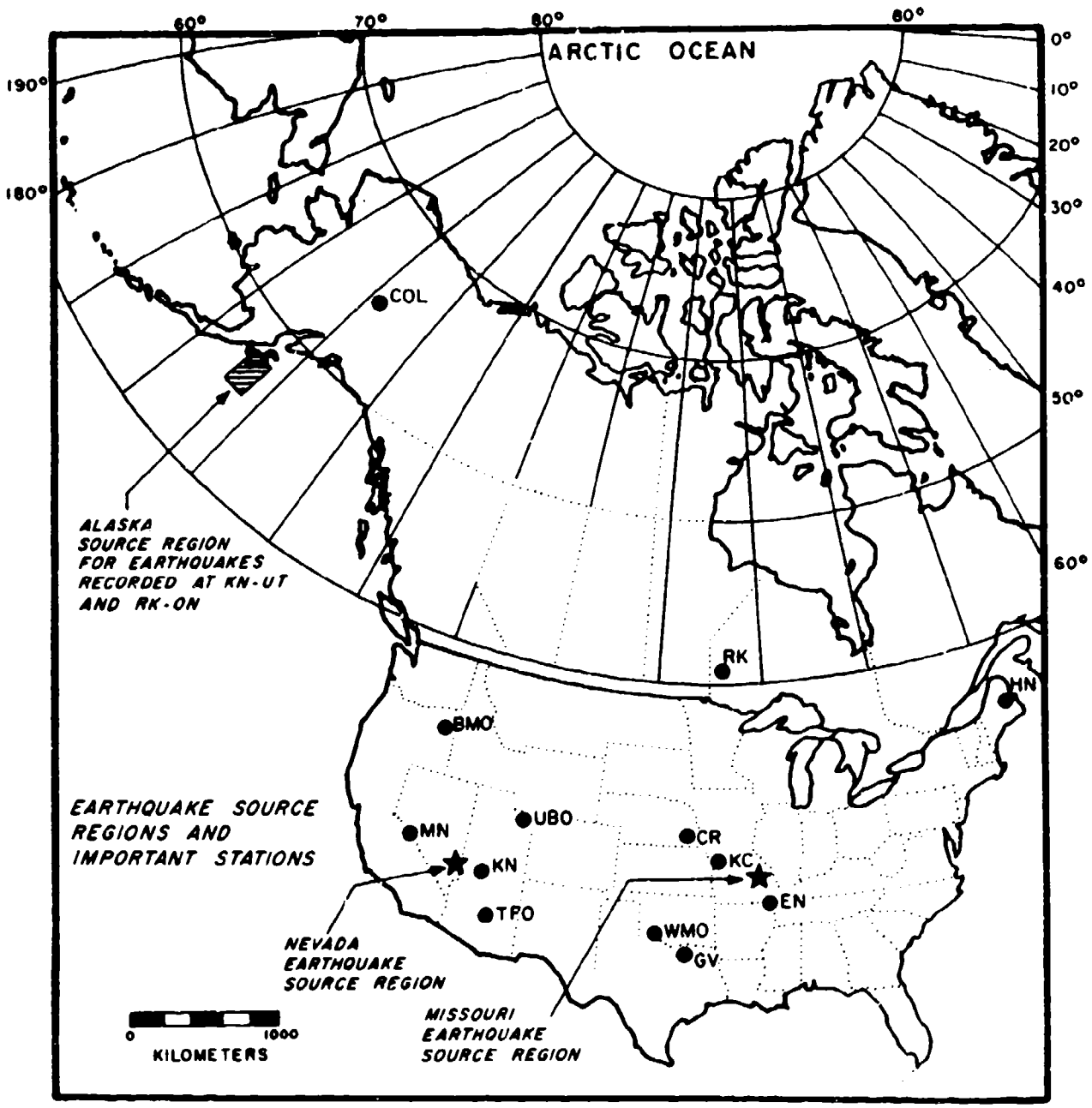

Figure 6. Earthquake source regions and important stations.

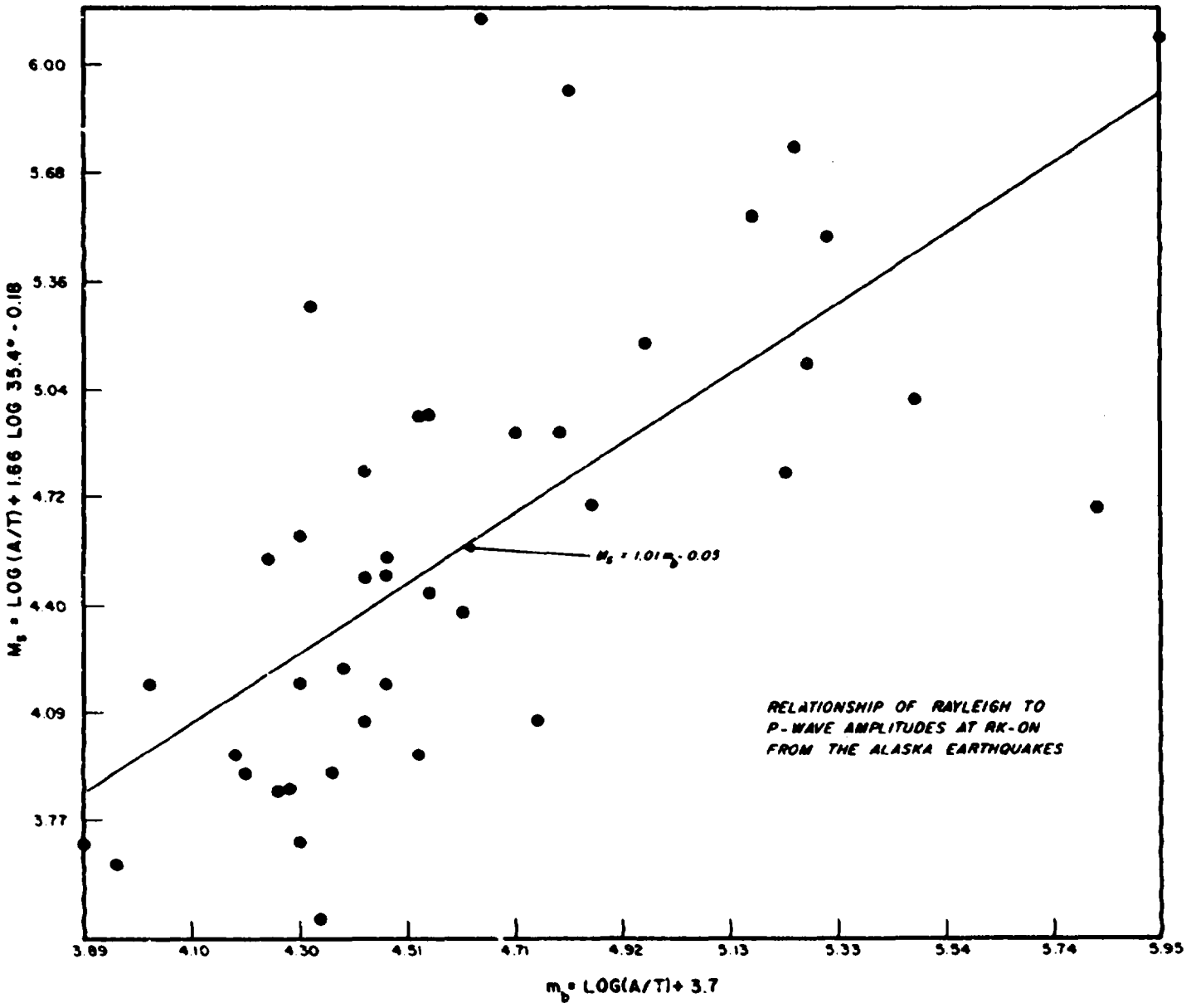

Figure 7. Relationship of Rayleigh wave amplitudes to P-wave amplitudes at RK-ON from Alaska earthquakes.

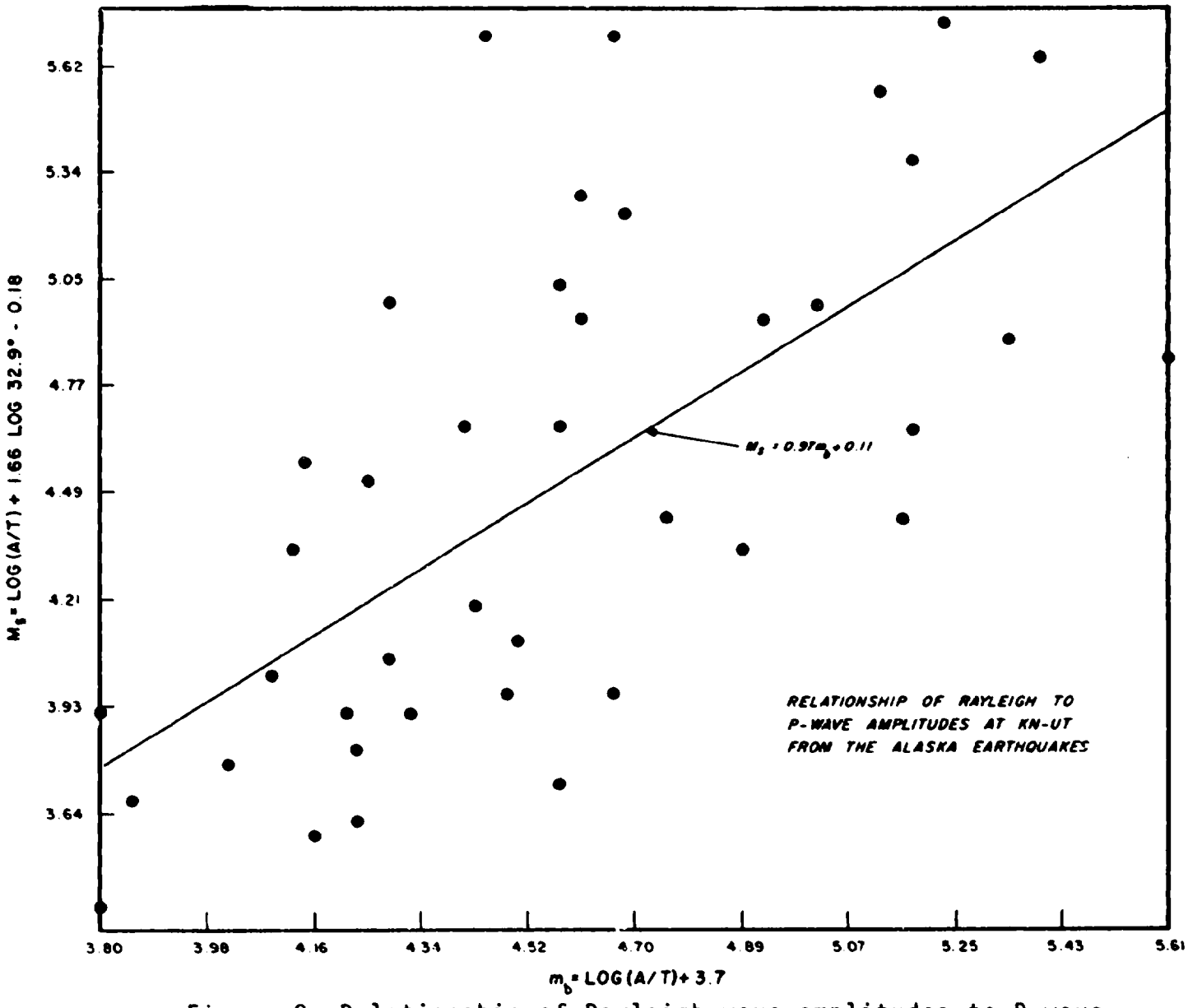

Figure 8. Relationship of Rayleigh wave amplitudes to P-wave amplitudes at KN-UT from Alaska earthquakes.

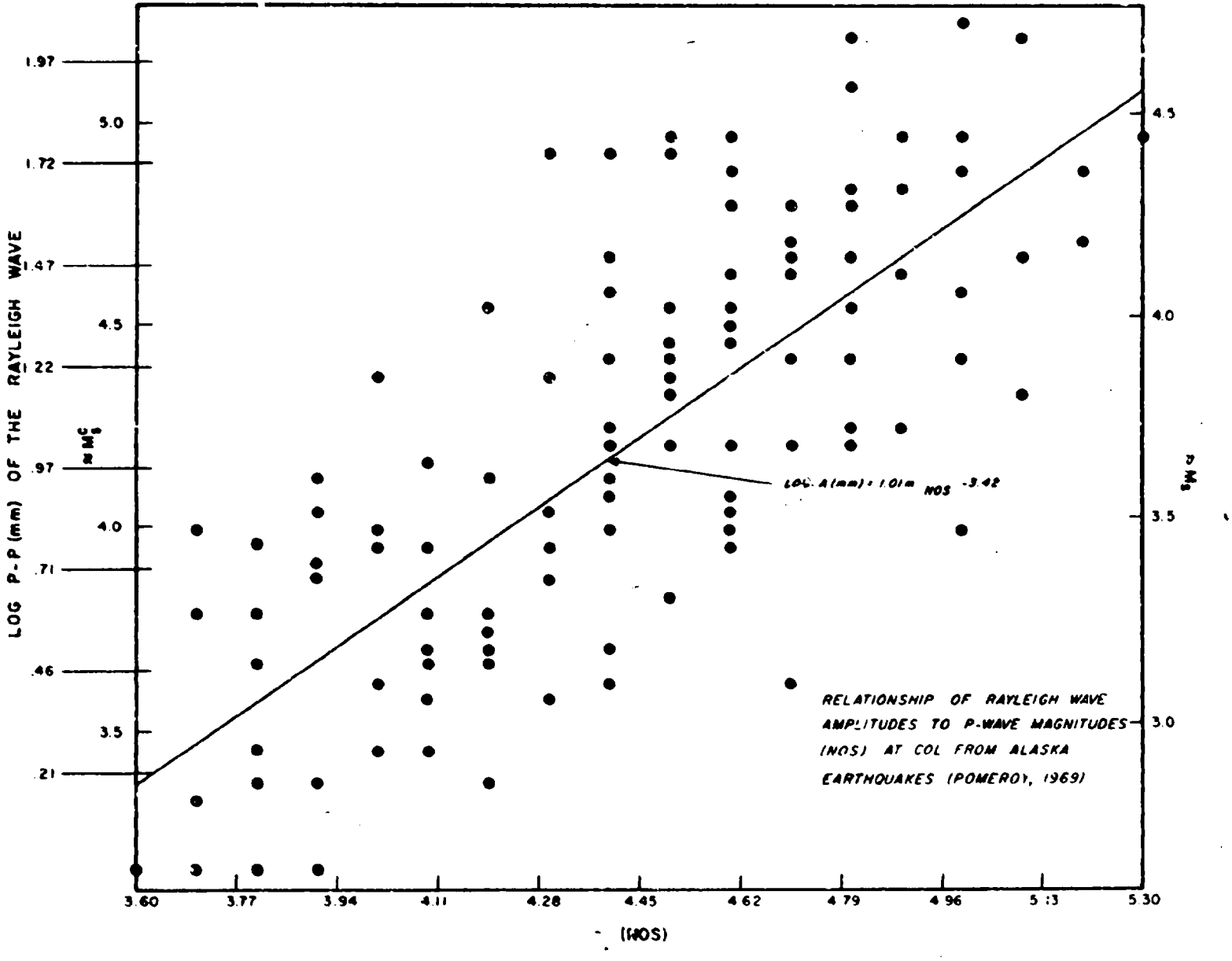

Figure 9. Relationship of Rayleigh wave amplitudes to P-wave magnitudes (NOS) at COL from Alaska earthquakes (Pomeroy, 1967).

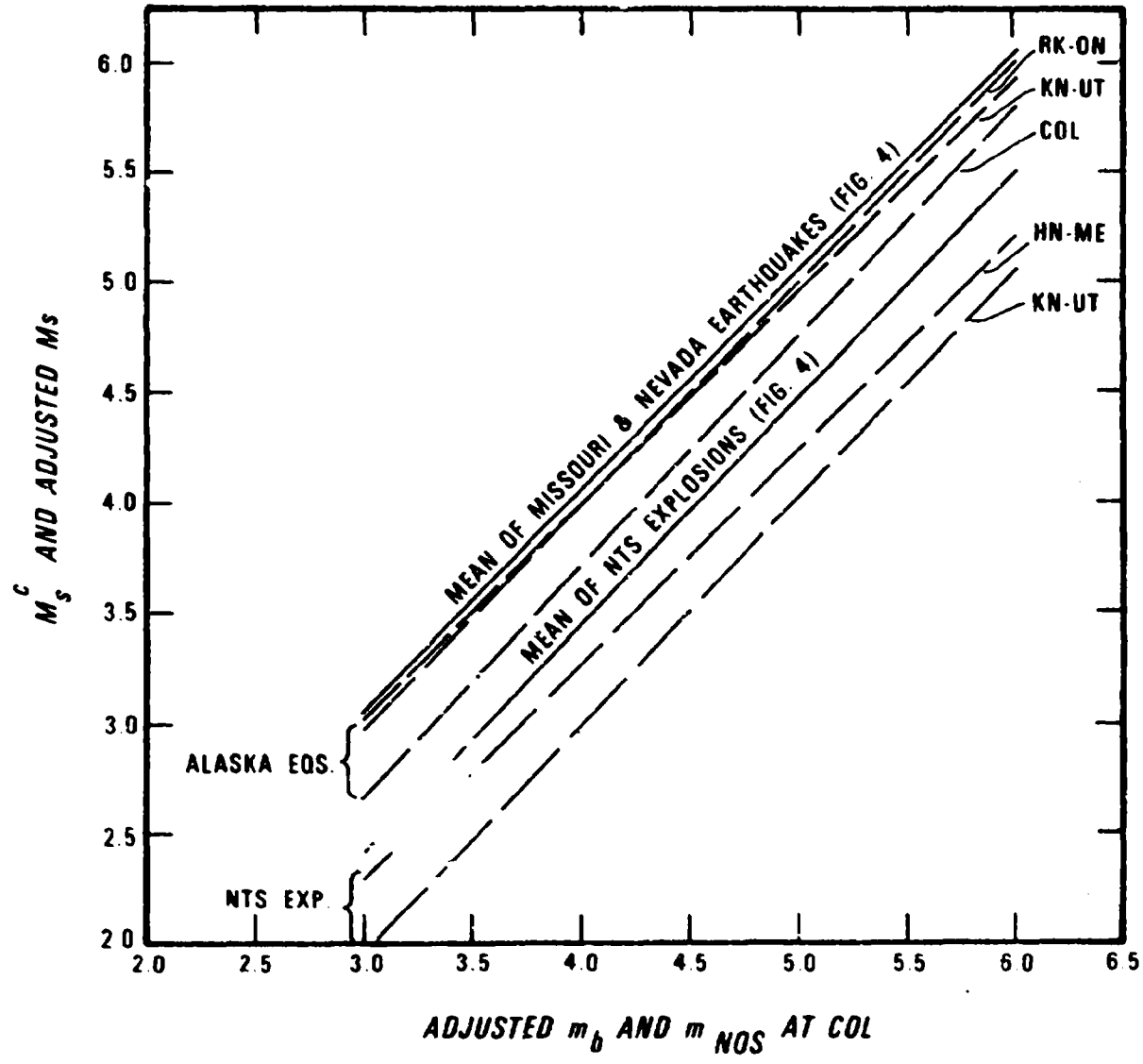

Figure 10. Summary of least square fits to individual and many station magnitude determinations for Alaska, Missouri, and Nevada source regions.

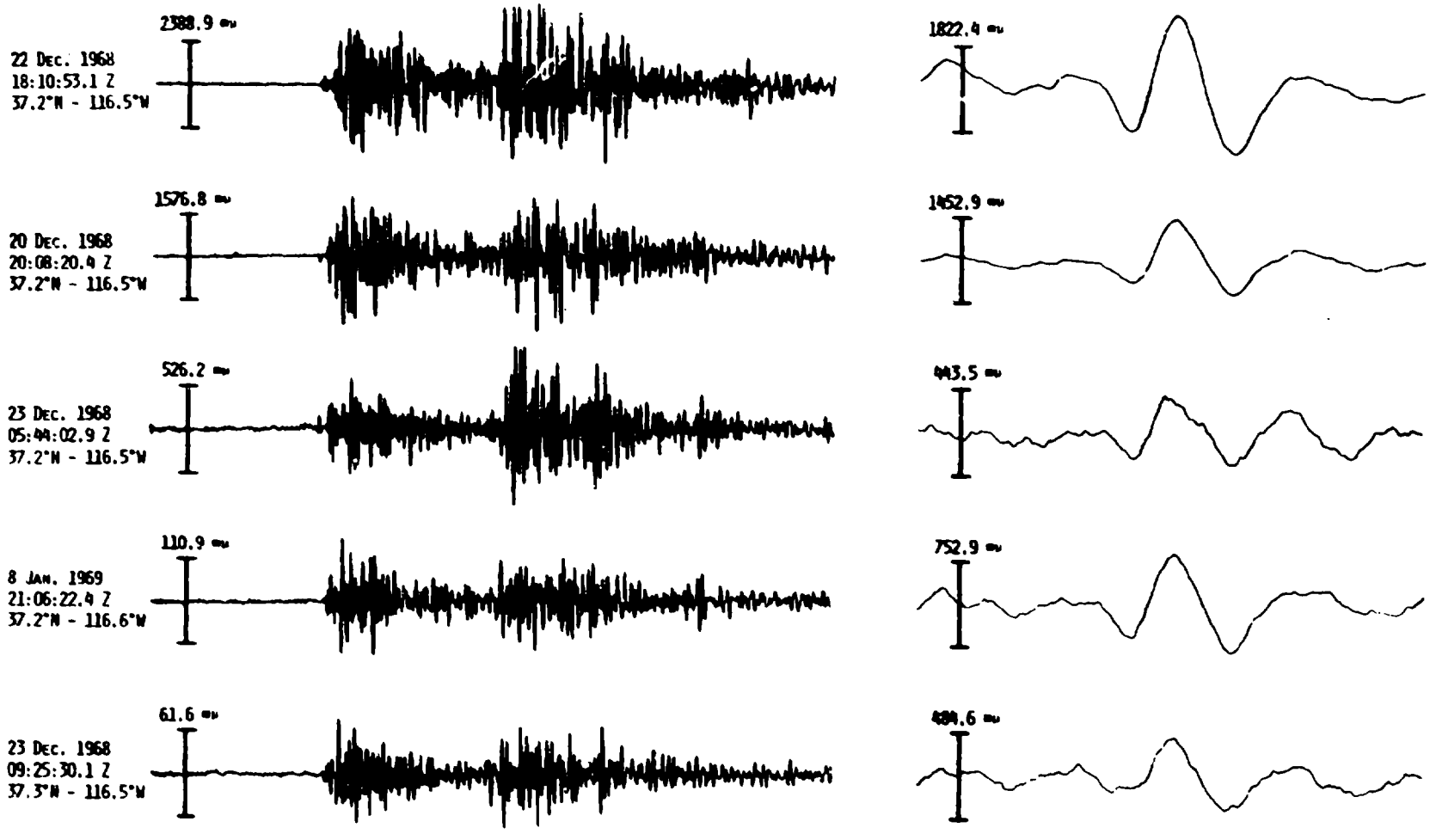

Figure 11. Seismic signals for earthquakes at MN-NV.

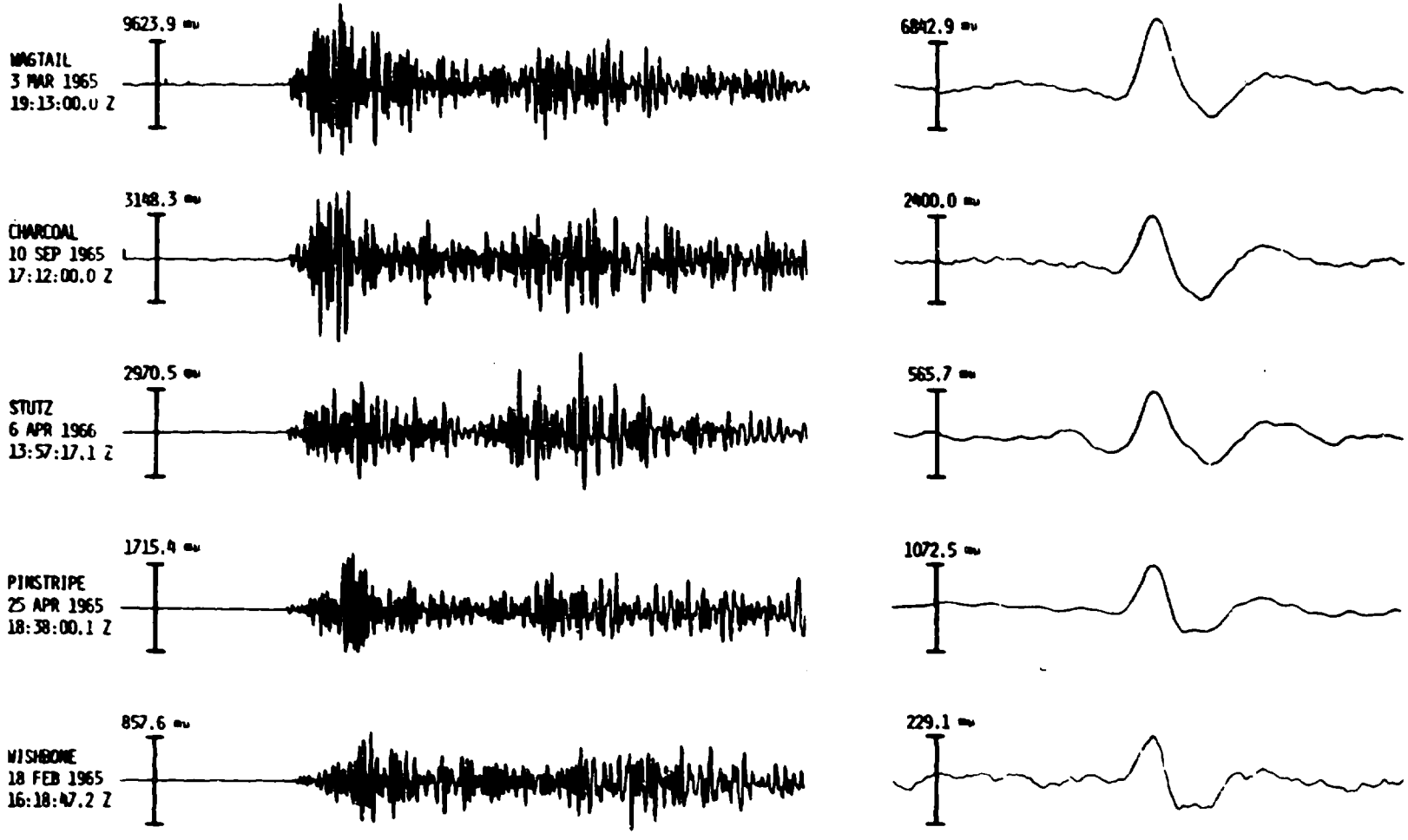

Figure 12. Seismic signals for explosions at MN-NV.

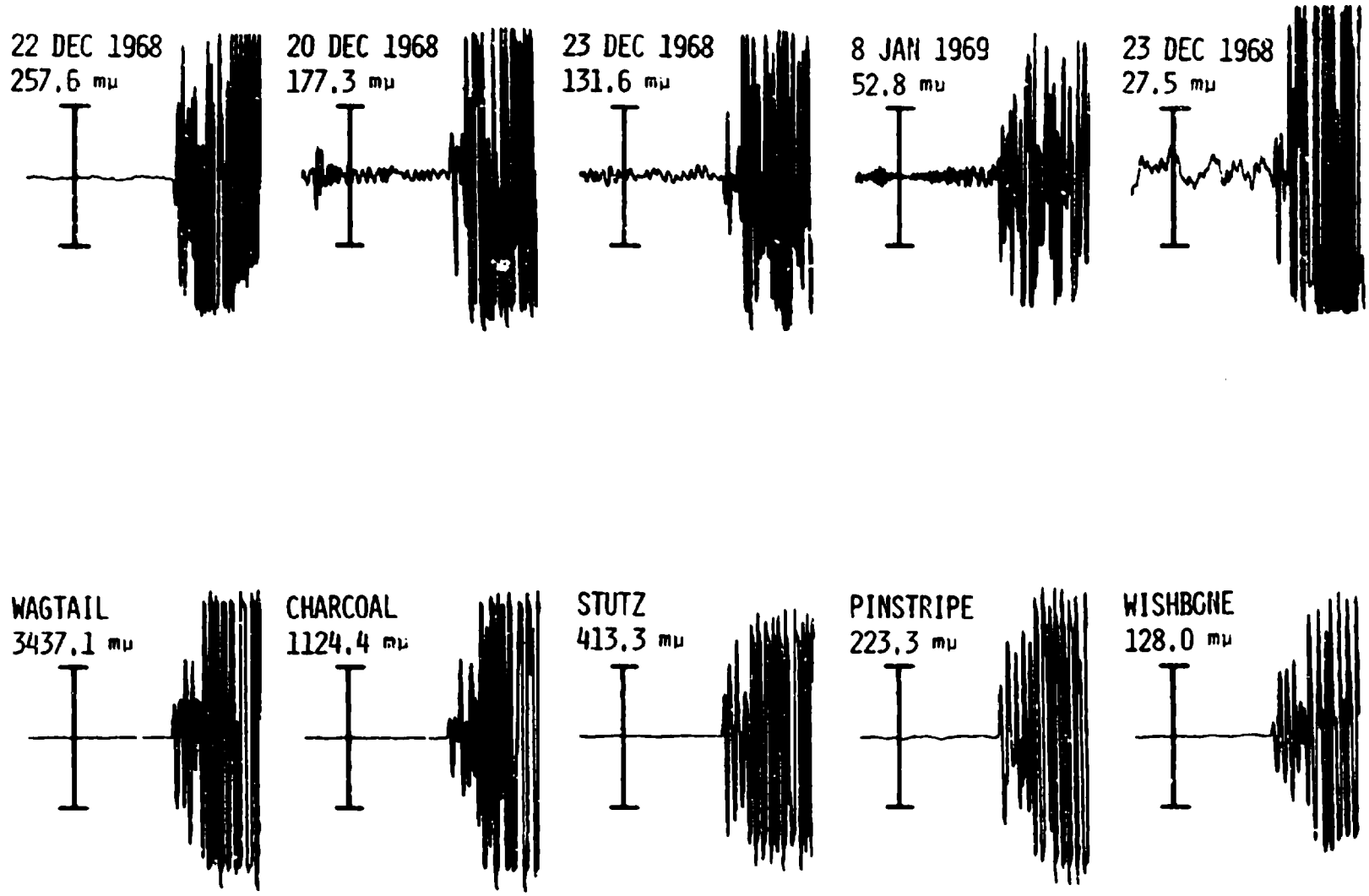

Figure 13. Short-period signals for earthquakes and explosions at higher gains at MN-NV.

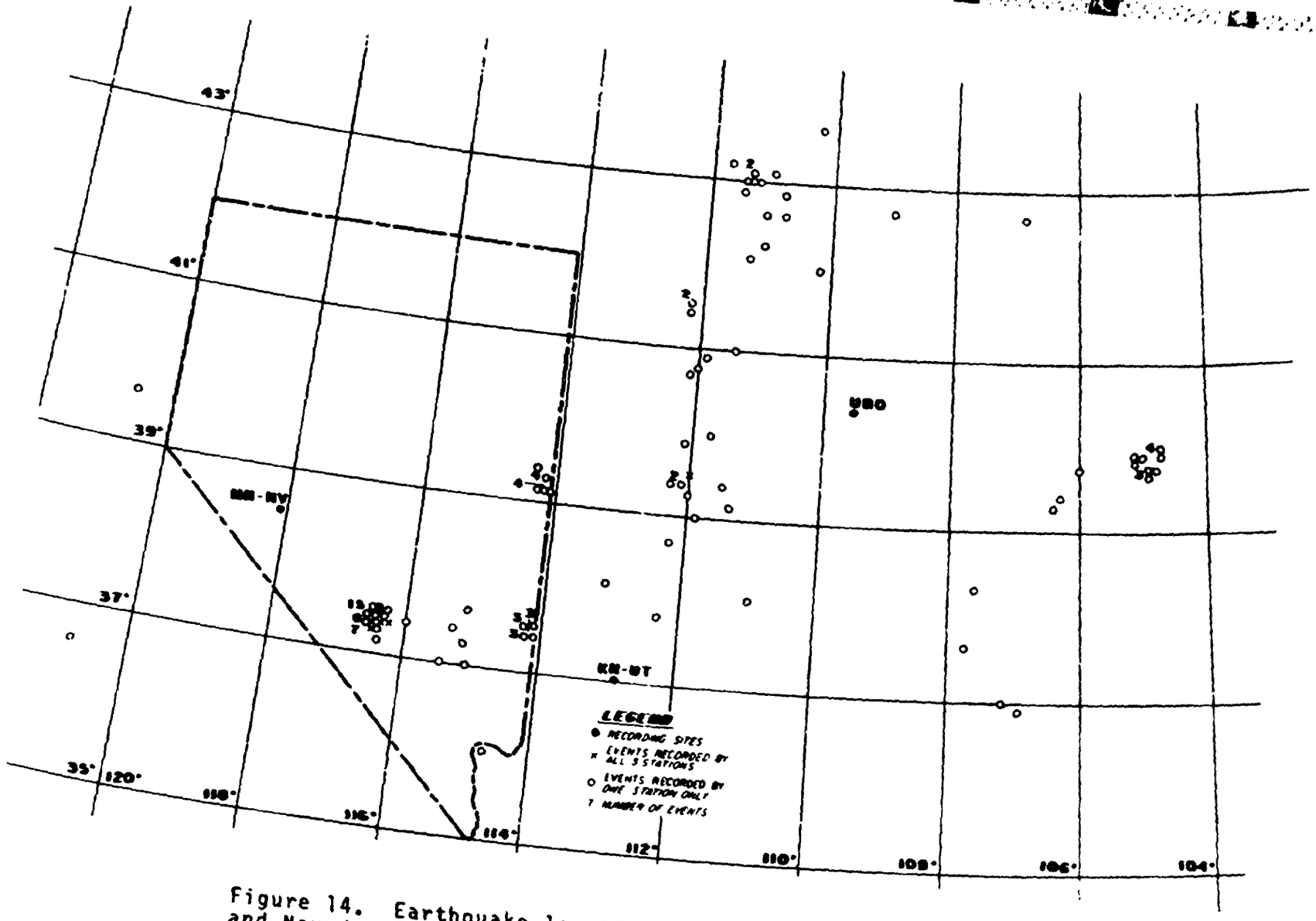

Figure 14. Earthquake locations relative to the stations and Nevada.

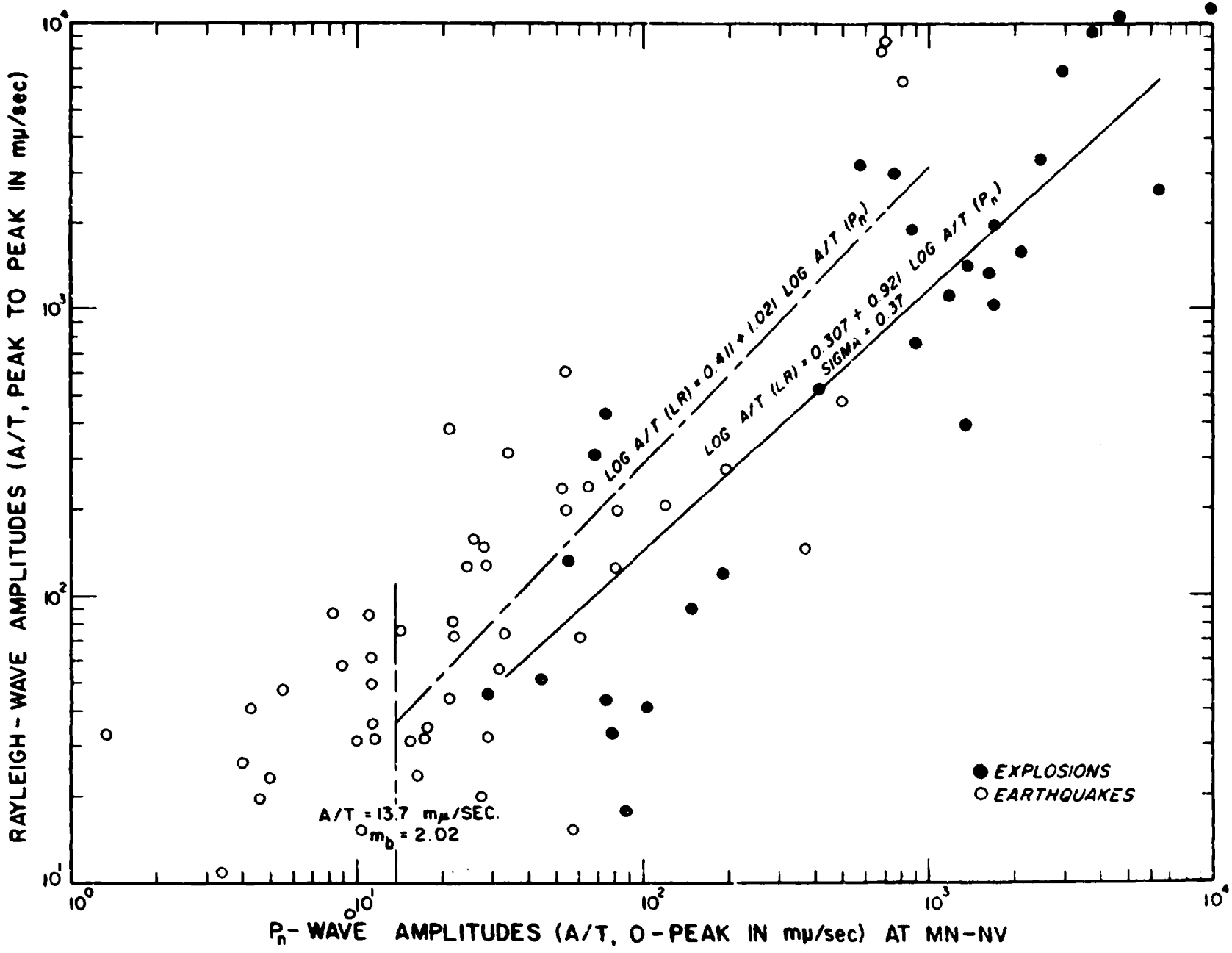

Figure 15. Rayleigh and Pn-wave amplitudes at MN-NV for Nevada earthquakes and explosions.

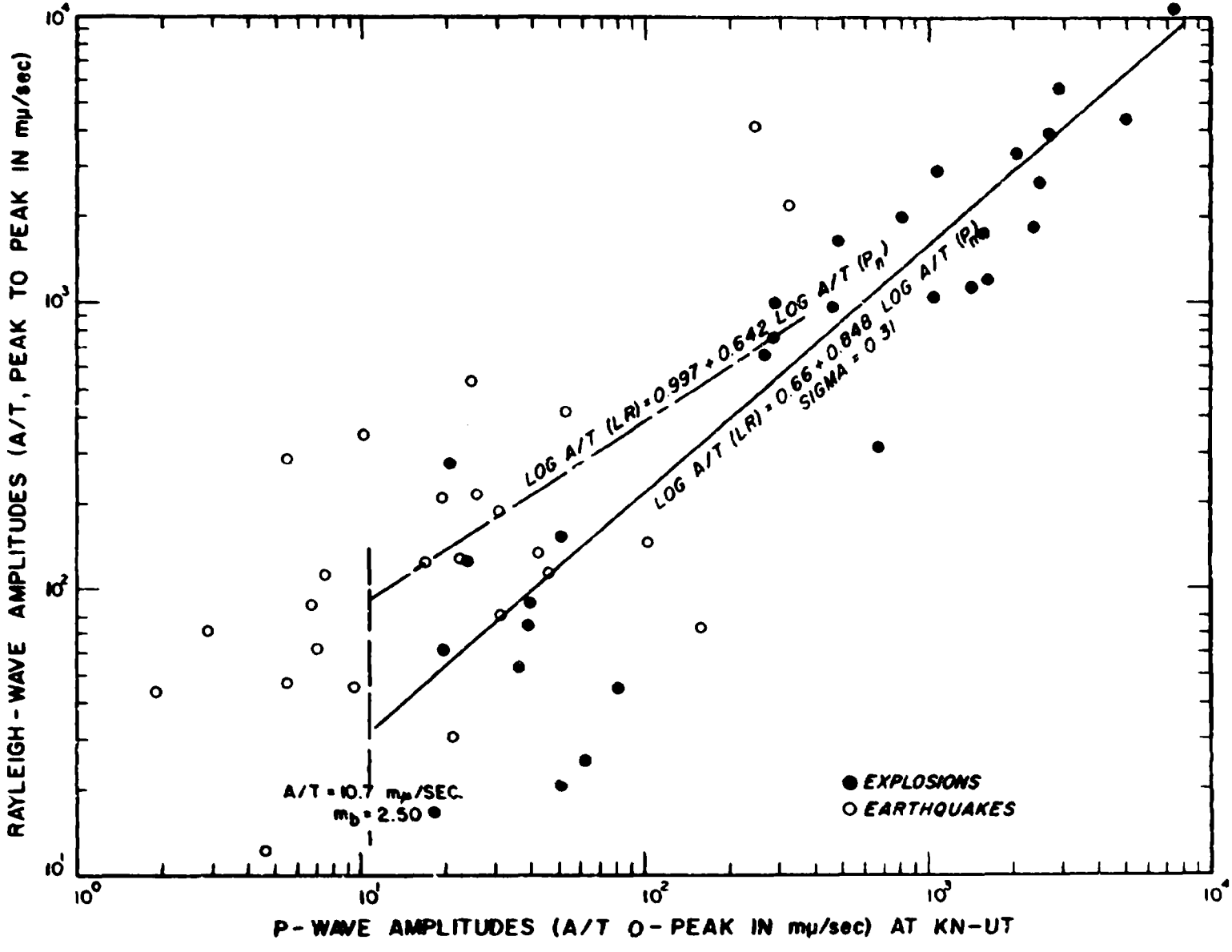

Figure 16. Rayleigh and Pn-wave amplitudes at KN-UT for Nevada earthquakes and explosions.

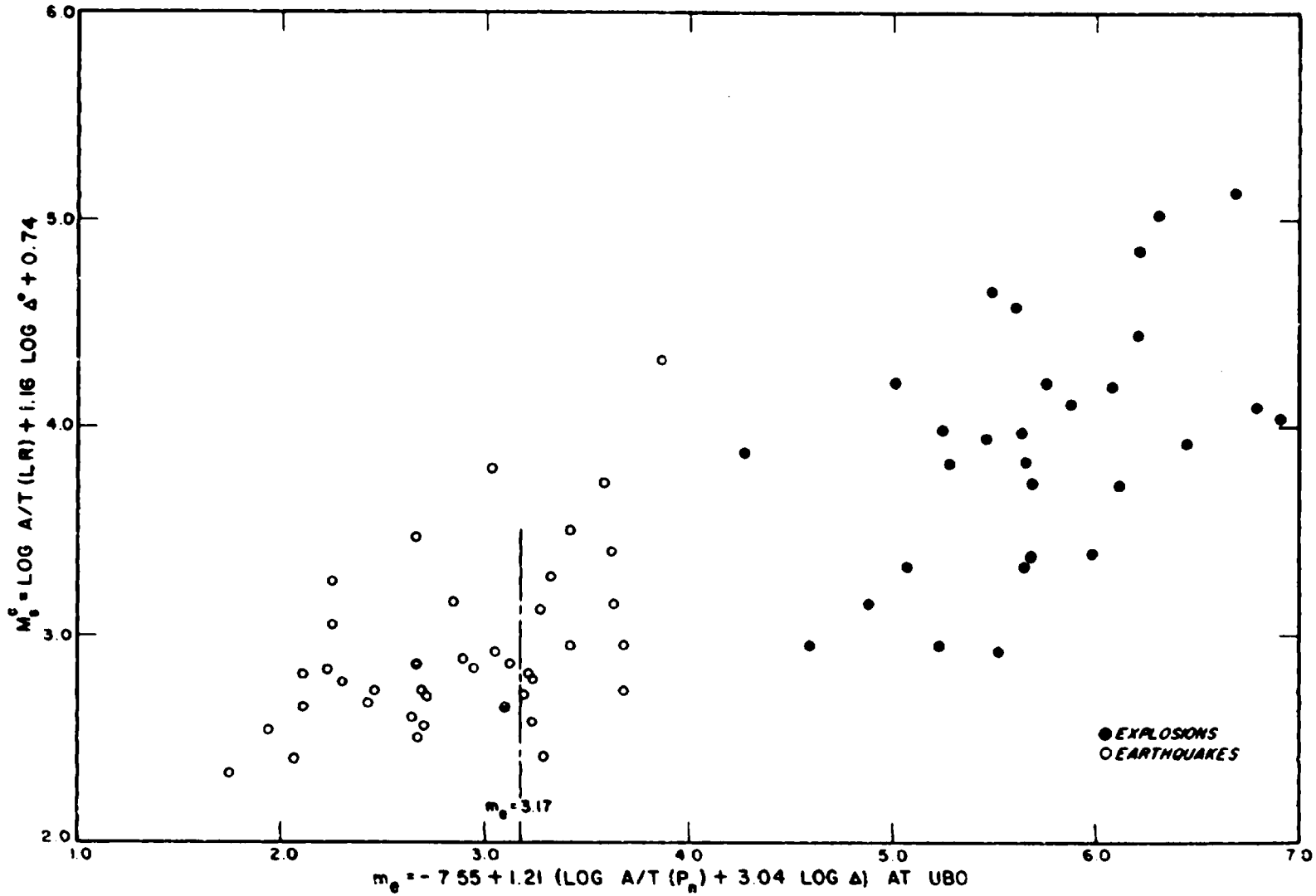

Figure 17. Surface and body wave magnitudes at UBO for Nevada earthquakes and explosions.

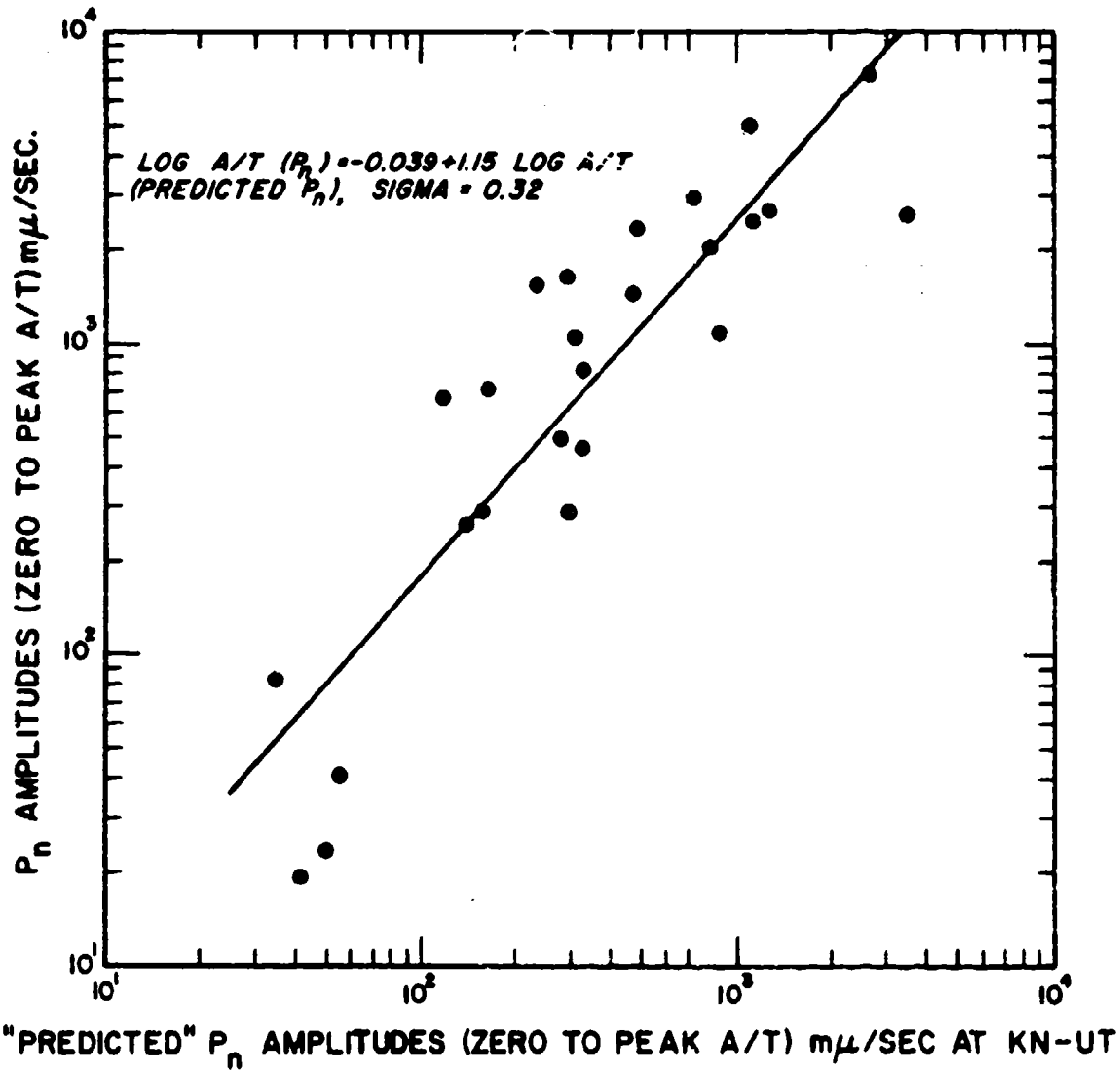

Figure 18. Pn amplitudes versus predicted Pn amplitudes at KN-UT.

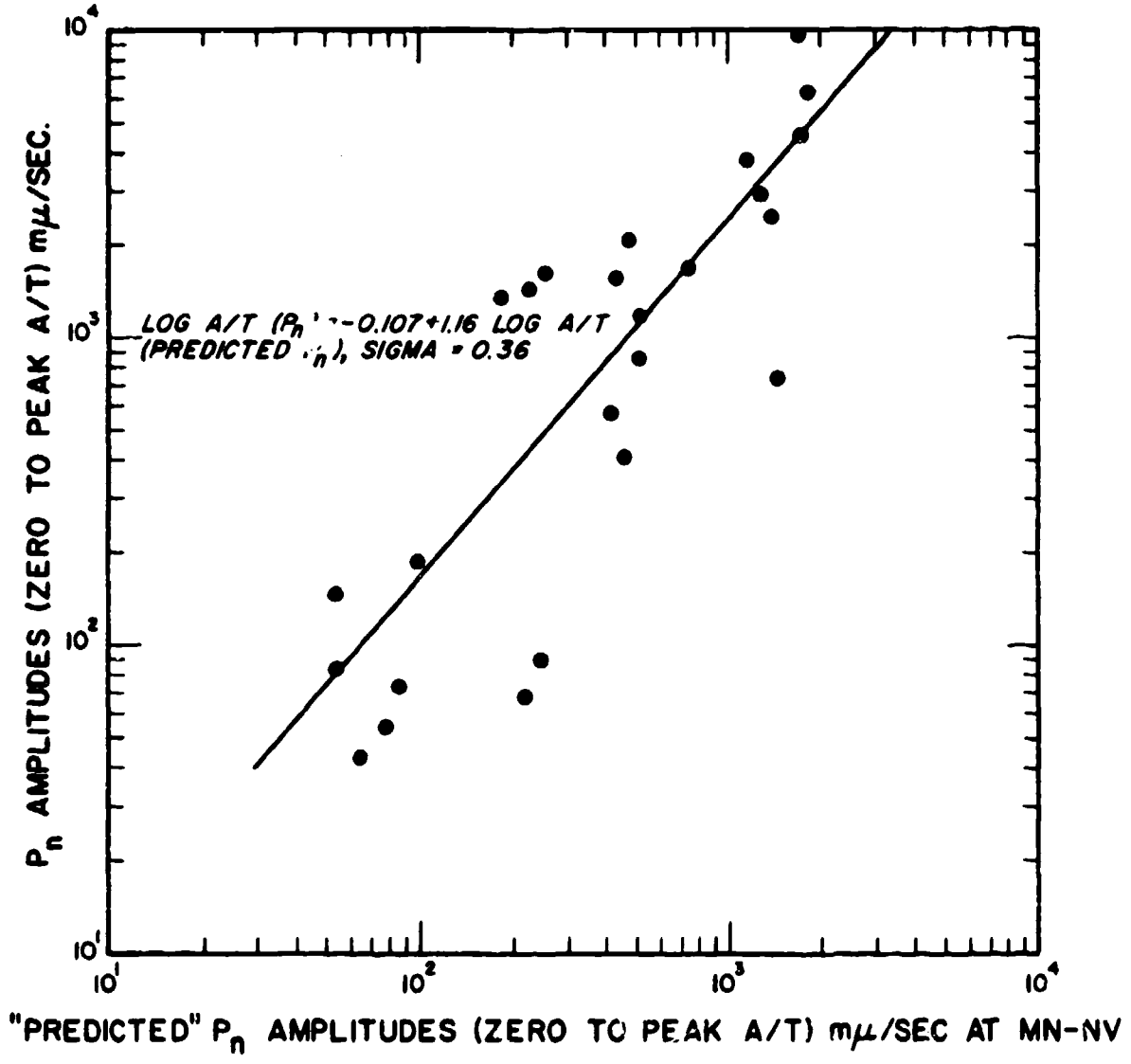

Figure 19. Pn amplitudes versus predicted Pn amplitudes at MN-NV.

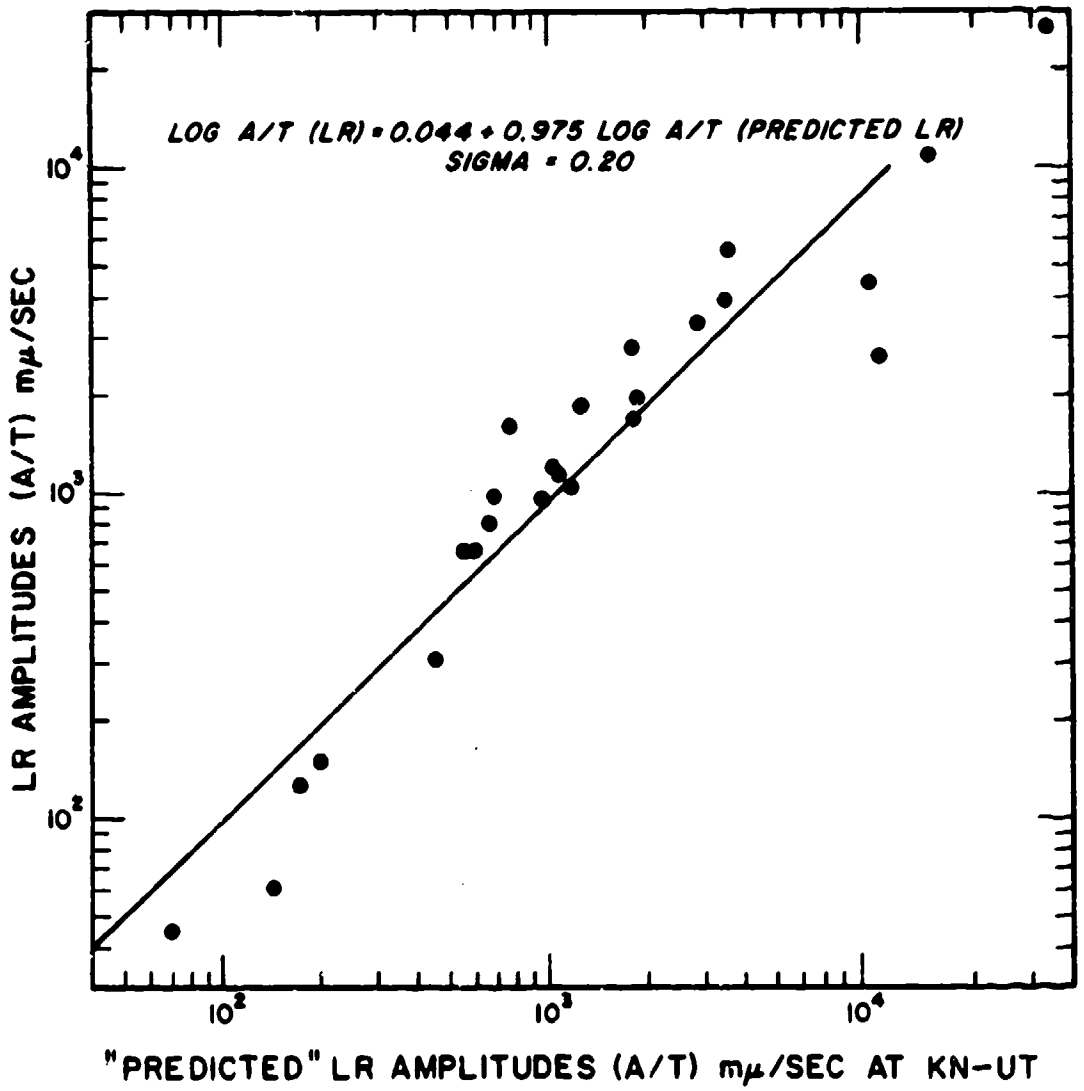

Figure 20. LR amplitudes versus predicted LR amplitudes at KN-UT.

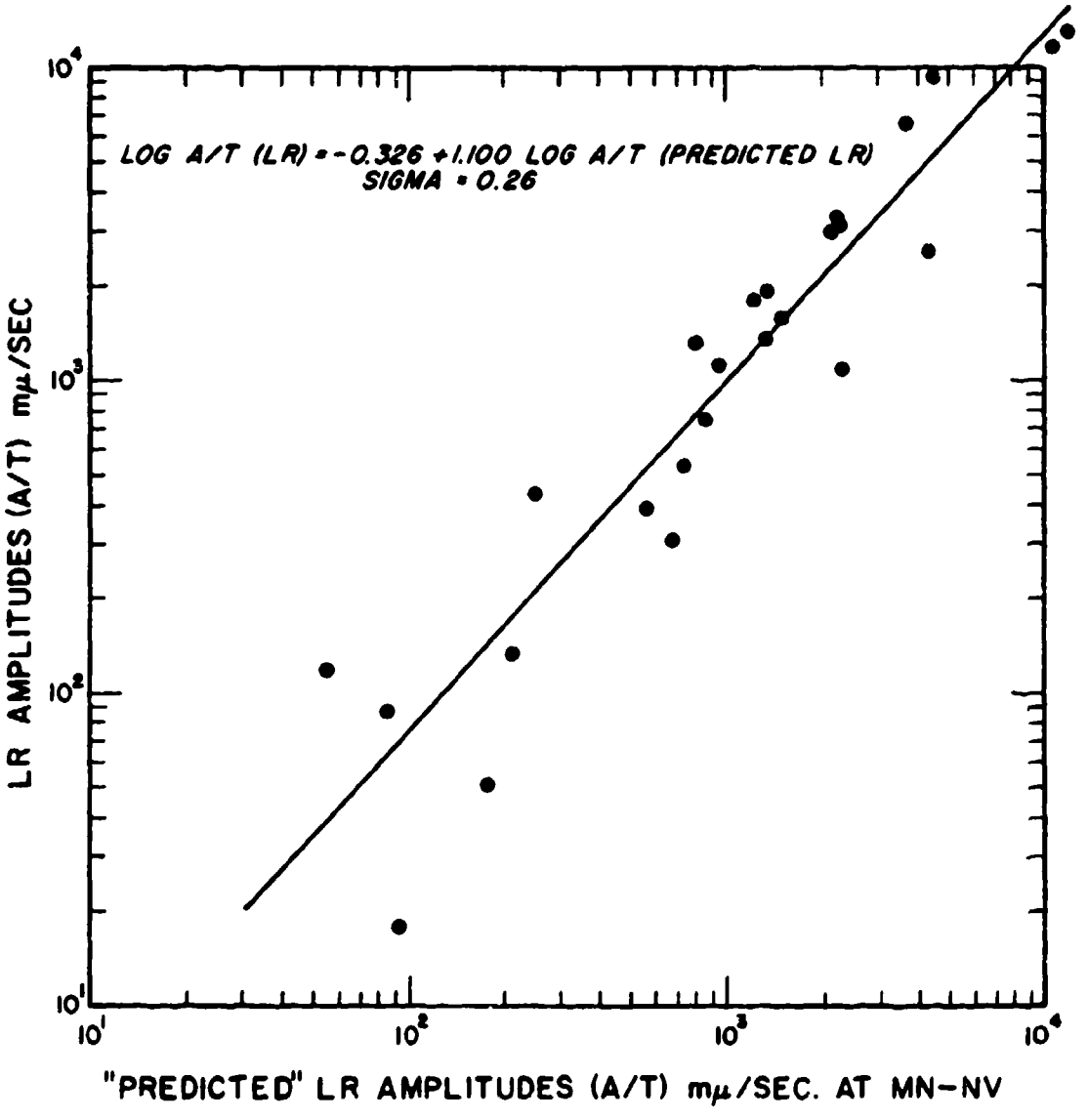

Figure 21. LR amplitudes versus predicted LR amplitudes at MN-NV.

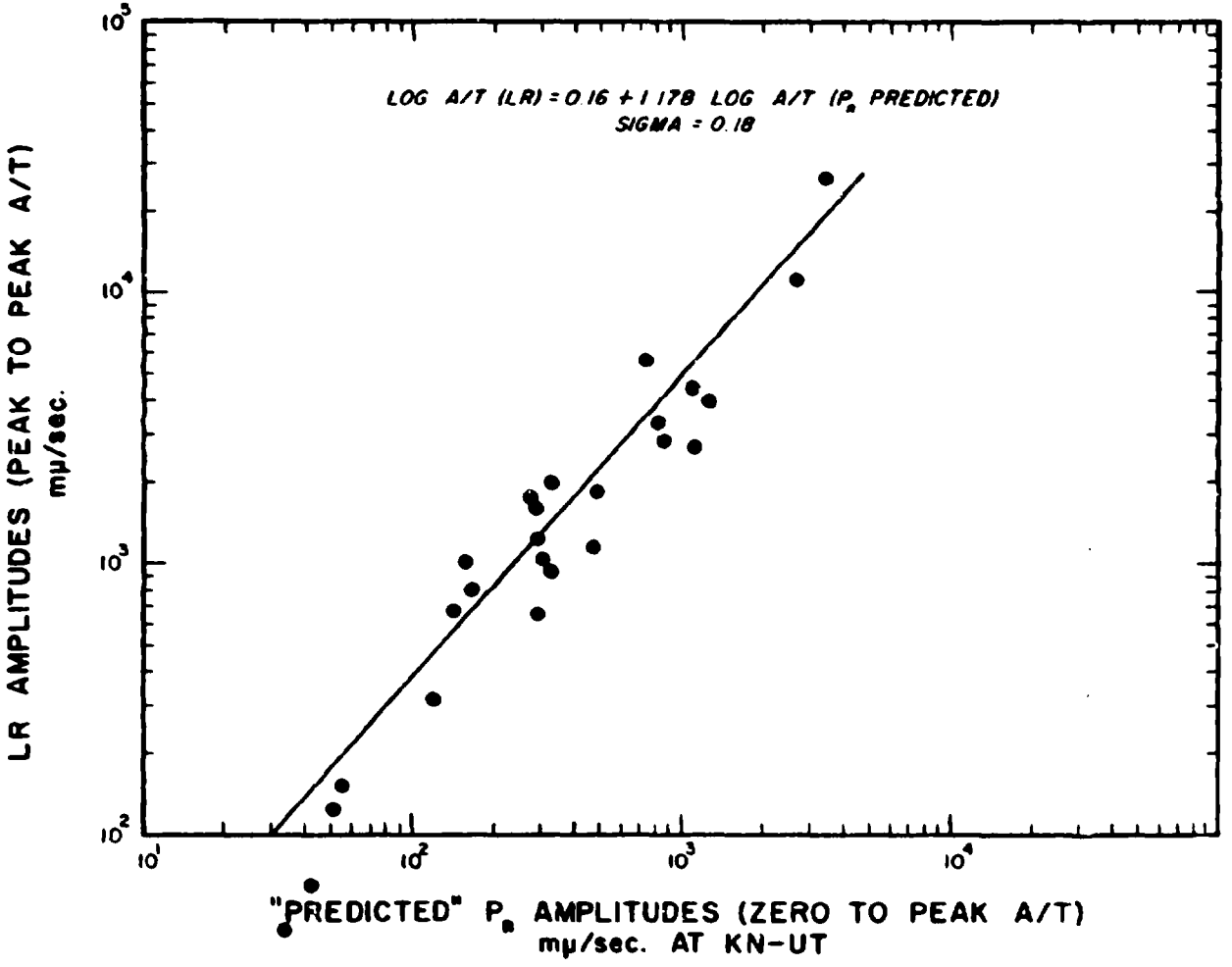

Figure 22. LR amplitudes versus predicted Pn amplitudes at KN-UT.

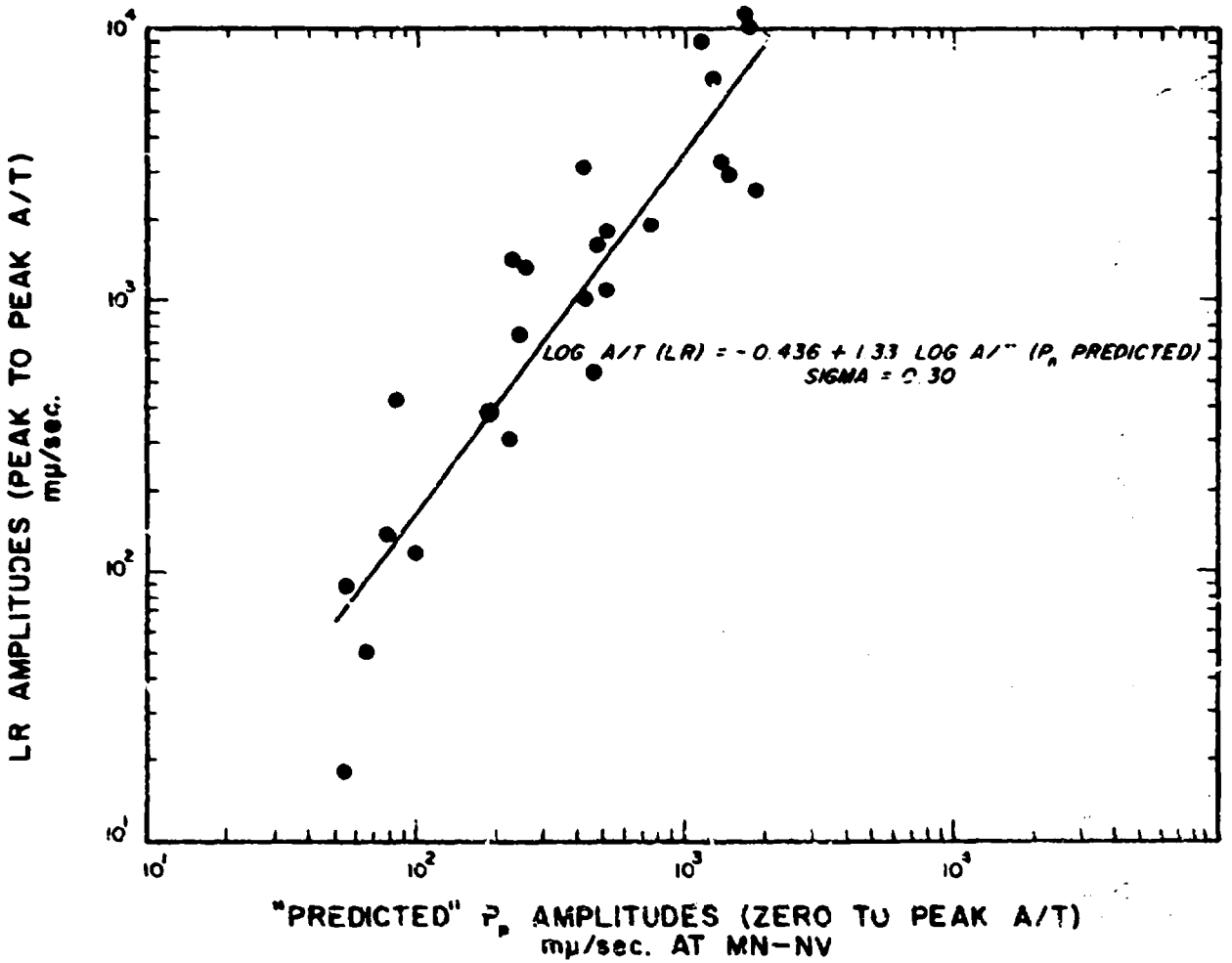

Figure 23. LR amplitudes versus predicted Pn amplitudes at MN-NV.

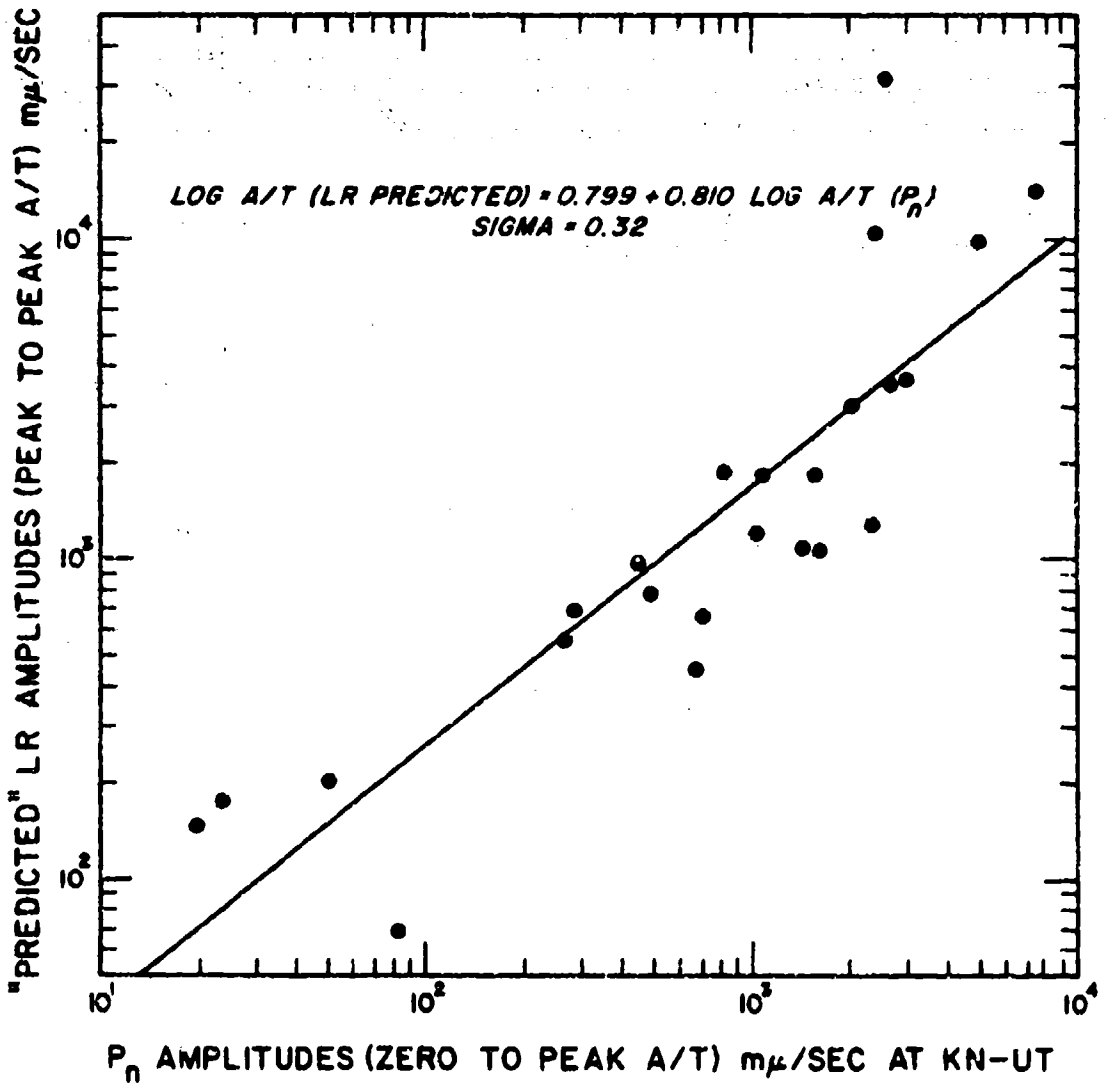

Figure 24. Predicted LR amplitudes versus Pn amplitudes at KN-UT.

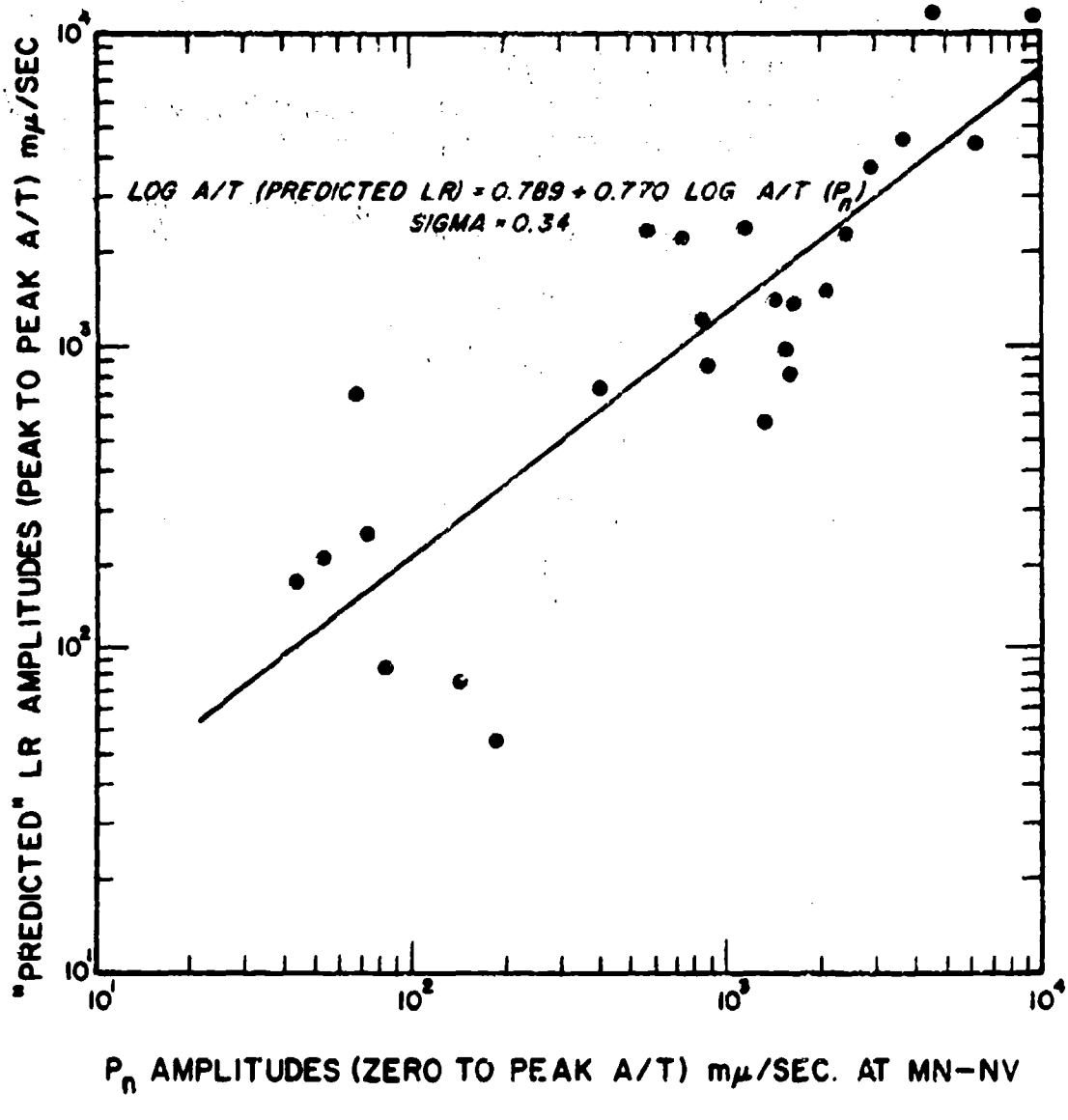

Figure 25. Predicted LR amplitudes versus Pn amplitudes at MN-NV.

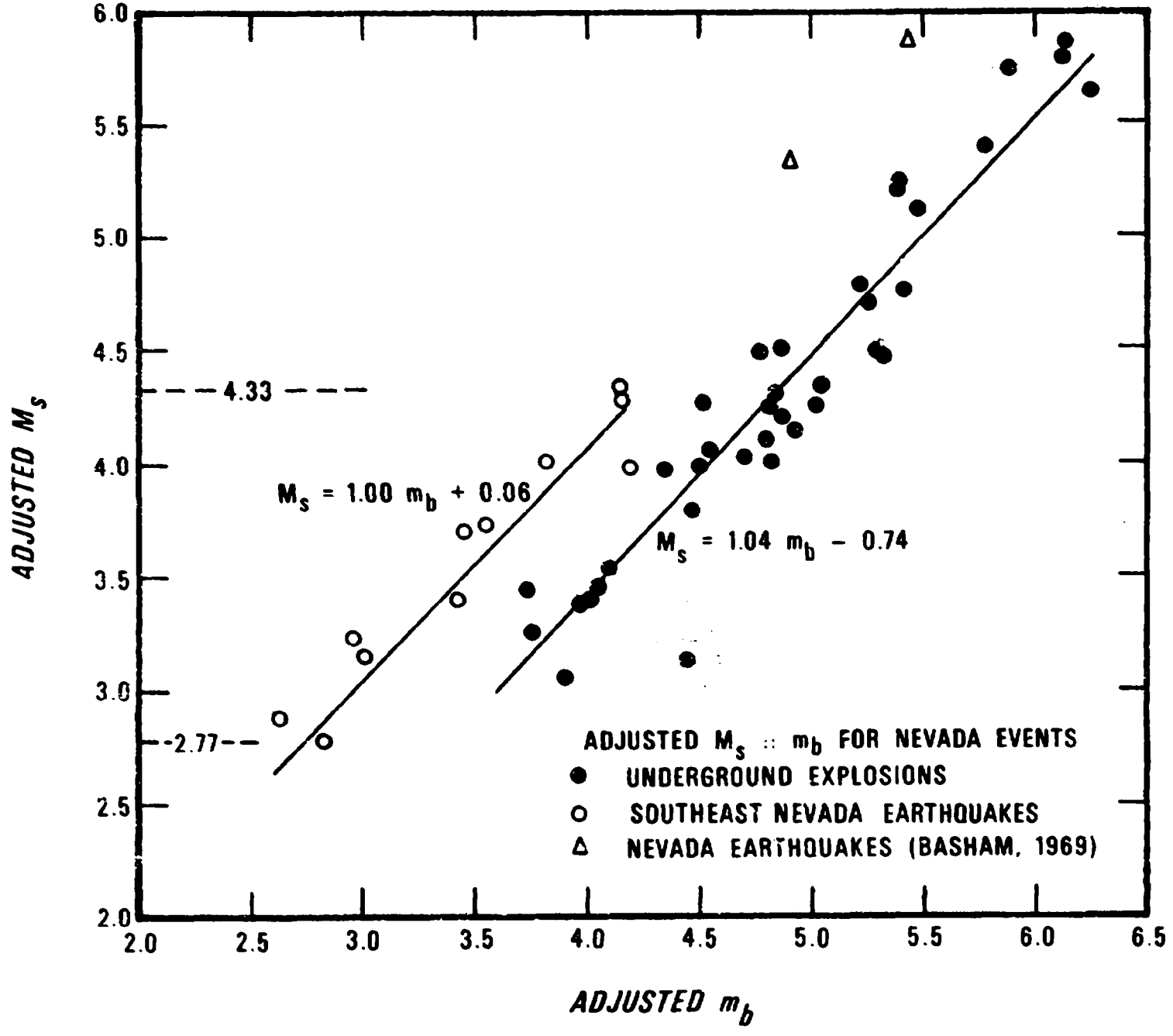

Figure 26. Adjusted M_s versus m_b for Nevada events.

TABLE 1

MAGNITUDES OF NEVADA TEST SITE EXPLOSIONS

NAME	DATE Day	Mo.	Yr.	ADJUSTED m_b	S.D.	n	M_s	S.D.	n	ADJUSTED M_s	S.D.	GEOLOGIC MEDIUM
AUK	2	10	64	4.50	0.51	31	3.52	0.35	21	3.97	0.21	TUFF
BENHAM	19	12	68	5.89	1.11	6	5.52	0.48	8	5.72	0.25	TUFF
BILBY	13	9	63	5.48	0.46	41	4.77	0.27	27	5.12	0.20	TUFF
BOURBON	20	1	67	4.78	0.56	14	4.19	0.42	13	4.49	0.30	LIMESTONE
BOXCAR	26	4	68	6.14	0.40	19	5.42	0.47	16	5.86	0.35	RHYOLITE
BRONZE	23	7	65	4.87	0.48	31	4.14	0.38	28	4.50	0.26	TUFF
BUFF	16	12	65	4.87	0.43	25	4.00	0.32	20	4.21	0.22	TUFF
CHARCOAL	10	9	65	4.82	0.29	19	3.54	0.32	17	4.00	0.19	TUFF
CHARTREUSE	6	5	66	5.04	0.57	21	4.11	0.24	18	4.33	0.21	RHYOLITE
CLIMAX	23	5	64	3.59	0.58	13	2.36	0.27	9	2.91	0.17	MASSIVE GRANITE
COMMODORE	20	5	67	5.40	0.55	20	5.02	0.29	17	5.24	0.26	TUFF
CORDUROY	3	12	65	5.42	0.37	28	4.53	0.34	21	4.77	0.20	TUFF
CUP	26	3	65	4.84	0.34	30	3.93	0.33	24	4.30	0.14	TUFF
DES MOINES	13	6	62	3.89	0.39	9	3.39	0	1	4.10	0	TUFF
DILUTED WATERS	16	6	65	4.05	0.49	23	2.87	0.29	15	3.46	0.30	ALLUVIUM
DUMONT	19	5	66	5.27	0.50	22	4.47	0.30	18	4.69	0.23	TUFF
DURYEA	14	4	66	4.82	0.43	21	4.00	0.40	17	4.25	0.26	RHYOLITE
FAULTLESS	19	1	68	6.25	0.23	18	5.60	0.37	12	5.64	0.31	TUFF (WATER SAT
FISHER	3	12	61	3.65	0.41	21	2.61	0	1	3.21	0	ALLUVIUM
FOXE	16	1	64	4.80	0.46	40	3.75	0.40	27	4.11	0.24	TUFF
GREELEY	20	12	66	6.13	0.38	22	5.62	0.38	21	5.79	0.33	ZEOLITIZED TUFF
HARDHAT	15	2	62	4.43	0.84	36	3.17	.42	1	3.74	.28	GRANITE
HAYMAKER	27	6	62	4.34	0.57	18	3.59	0.37	16	3.98	0.24	ALLUVIUM
HALFBEAK	30	9	66	5.78	0.51	21	5.23	0.37	17	5.39	0.30	RHYOLITE
KLICKITAT	20	2	64	4.57	0.51	34	3.65	0.36	25	4.04	0.20	TUFF
KNICKERBOCKER	26	5	67	5.22	0.36	14	4.49	0.35	13	4.78	0.31	RHYOLITE
MADISON	12	12	62	3.89	0.46	18	3.31	0.42	3	3.89	0.30	TUFF
MARSHMALLOW	28	6	62	4.01	0.31	21	2.76	0.45	6	3.39	0.45	TUFF
MERRIMAC	13	7	62	3.73	0.51	15	2.84	0.41	7	3.45	0.31	ALLUVIUM
MINK	29	10	61	2.93	0.17	6	2.16	0	1	2.67	0	ALLUVIUM
MISSISSIPPI	5	10	62	4.70	0.43	53	3.71	0.35	35	4.02	0.25	TUFF
NASH	19	1	67	4.93	0.54	15	3.63	0.55	7	4.14	0.44	TUFF
PALANQUIN	14	4	65	3.75	0.30	18	2.67	0.30	10	3.26	0.25	RHYOLITE
PAMPAS	1	3	62	3.74	0.33	19	2.74	0.47	2	3.54	0.35	ALLUVIUM
PAR	9	10	64	4.44	0.41	32	2.55	0.25	17	3.13	0.23	TUFF
PILEDRIVER	2	6	66	5.32	0.57	22	4.24	0.42	18	4.47	0.29	GRANITE
PINSTRIPE	25	4	66	4.09	0.58	15	3.27	0.42	12	3.53	0.23	TUFF
RED HOT	5	3	66	3.47	0.45	11	2.28	0	1	3.05	0	TUFF
REX	24	2	66	4.52	0.40	21	4.00	0.51	9	4.27	0.25	TUFF
SCOTCH	23	5	67	5.39	0.52	21	4.99	0.40	18	5.21	0.31	RHYOLITE
SCROLL	23	4	68	3.89	0.46	15	2.41	0.64	6	3.06	0.57	VITRIC TUFF
SEDAN	6	7	62	4.07	0.55	17	3.56	0.36	21	3.96	0.19	ALLUVIUM
SMALLBOY	14	7	62	2.86	0.65	3	2.60	0	1	3.18	0	AIR
STUTZ	6	4	66	4.15	0.32	17	2.69	0.08	3	2.87	0.14	ALLUVIUM
TAN	3	6	66	5.30	0.44	22	4.27	0.32	21	4.48	0.23	TUFF
TURF	24	4	64	4.55	0.51	36	3.72	0.38	32	4.06	0.26	ALLUVIUM
WAGTAIL	3	3	65	5.03	0.51	32	3.84	0.32	19	4.26	0.14	TUFF
WISHBONE	18	2	65	3.97	0.43	32	2.78	0.29	12	3.38	0.27	ALLUVIUM

TABLE II

MAGNITUDES NEVADA AND MISSOURI EARTHQUAKES

DATE	TIME(Z)	LAT.	LONG.	DEPTH	m_{NOS}	LOCATION	Adjusted m_b	S.D.	n	ADJUSTED M_s	S.D.	n	M_s	S.D.
21 Oct. 65	0204:38.3	37.5N	91.0W	22	5.2	E. Missouri	3.96	0.42	8	3.91	0.33	13	3.72	0.41
13 Feb. 66	2319:36.9	37.1N	91.0W	7	4.7	E. Missouri	3.29	0.31	6	3.25	0.31	3	3.00	0.51
17 Aug. 66	0237:02.0	37.4N	114.1W	33	–	S. Nevada	2.02	0.04	2	2.22	0	1	1.64	0
17 Aug. 66	0414:00.9	37.4N	114.2W	33	–	S. Nevada	2.83	0.13	4	2.77	0.41	4	2.08	0.48
17 Aug. 66	0446:41.2	37.4N	114.1W	33	–	S. Nevada	2.63	0.41	4	2.87	0.43	3	2.16	0.54
17 Aug. 66	1119:06.0	37.4N	114.1W	33	–	S. Nevada	2.38	0.38	2	2.91	0	1	2.25	0
17 Aug. 66	1914:77.7	37.3N	114.1W	33	–	S. Nevada	2.96	0.54	4	3.22	0.71	4	2.55	0.86
17 Aug. 66	2307:58.9	37.3N	114.1W	33	5.2	S. Nevada	4.15	0.45	13	4.27	0.31	12	3.90	0.39
18 Aug. 66	0614:58.6	37.4N	114.1W	9	4.7	S. Nevada	3.00	0.57	5	3.15	0.68	4	2.46	0.79
18 Aug. 66	0627:44.0	37.3N	114.2W	33	–	S. Nevada	2.78	0.61	4	2.13	0.05	2	1.37	0.24
18 Aug. 66	0803:37.0	37.4N	114.1W	33	–	S. Nevada	2.27	0.18	4	2.08	0	1	1.19	0
18 Aug. 66	0915:34.9	37.3N	114.1W	9	5.1	S. Nevada	4.14	0.53	15	4.31	0.32	16	4.05	0.47
18 Aug. 66	1009:22.6	37.3N	114.3W	33	–	S. Nevada	2.95	0.45	4	3.00	0.55	3	[illegible]	0.68
18 Aug. 66	1200:35.2	37.3N	114.2W	33	4.4	S. Nevada	3.42	0.27	8	3.40	0.40	[illegible]	[illegible]	0.26
18 Aug. 66	1333:20.8	37.4N	114.2W	33	4.6	S. Nevada	3.55	0.51	9	3.73	0.43	9	3.30	.47
18 Aug. 66	1735:06.4	37.4N	114.2W	33	5.2	S. Nevada	4.19	0.42	11	3.98	0.28	13	3.77	0.41
18 Aug. 66	2009:16.0	37.3N	114.3W	33	–	S. Nevada	2.75	0.41	4	2.52	0.20	2	1.77	0.39
19 Aug. 66	1051:38.5	37.4N	114.1W	11	4.5	S. Nevada	3.82	0.47	11	4.01	0.31	18	3.73	0.43
19 Aug. 66	1117:47.7	37.3N	114.2W	33	4.4	S. Nevada	2.94	0.79	5	3.13	0.37	8	2.57	0.46
22 Aug. 66	0827:30.2	37.3N	114.2W	33	4.8	S. Nevada	3.46	0.72	8	3.71	0.39	16	3.44	0.58

TABLE IIIA

Earthquake List for KN-NV

Date	Origin	North Latitude(°)	West Longitude(°)	O-P A/T P	O-P A/T LR	NOS m_b	Comment
18 Jun 65	08 14 01.0	37.3	116.0	10.8	43.2	3.4	
17 Aug 66	23 07 59.0	37.3	114.1	8.1	43.4	5.2	
18 Aug 66	09 15 34.9	37.3	114.1	27.3	73.9	5.1	
18 Aug 66	12 00 35.2	37.3	114.2	10.1	7.6	4.4	
18 Aug 66	17 35 06.4	37.4	114.2	30.9	27.7	5.2	
19 Aug 66	10 51 38.5	37.4	114.1	23.9	62.8	4.5	
22 Aug 66	08 27 30.2	37.3	114.2	34.5	36.9	4.8	
14 Sep 66	22 40 26.4	39.5	120.5	11.1	17.8	4.5	
22 Sep 66	19 59 40.2	37.3	114.1	20.6	22.2	4.7	
23 Sep 66	11 56 09.7	37.3	114.2	80.4	97.8	4.5	
21 Dec 66	02 14 26.8	37.4	116.5	8.7	28.6	3.5	
21 Dec 66	06 02 05.5	37.3	116.5	9.8	15.5	3.4	
21 Dec 66	14 37 29.6	37.3	116.4	16.0	11.8	3.6	
02 Jan 67	09 11 02.2	37.4	114.2	16.2	15.9	4.4	
16 Feb 67	15 05 53.1	37.4	114.2	17.3	17.4	4.5	
25 Mar 68	11 32 07.1	36.6	120.7	51.9	117.0	4.4	
26 Apr 68	15 32 21.0	37.2	116.5	696.0	4310.0	4.0	C w/KN-UT
26 Apr 68	16 35 17.0	37.2	116.5	808.0	3130.0	4.9	
28 Apr 68	04 23 40.0	37.2	116.5	59.0	35.6	4.0	C
28 Apr 68	16 35 17.0	37.1	116.4	25.2	7.6	3.7	
30 Apr 68	07 49 03.0	37.3	116.3	33.4	156.0	4.2	C
04 May 68	23 31 10.0	37.3	116.6	5.0	11.6	3.6	
04 May 68	23 28 45.0	37.2	116.4	3.3	5.4	3.7	
19 Dec 68	19 18 19.6	37.3	116.4	118.1	100.1	4.1	C
19 Dec 68	19 54 01.2	37.2	116.5	367.2	70.9	4.3	C
19 Dec 68	22 23 26.3	37.2	116.5	480.7	233.7	5.0	C
20 Dec 68	01 15 02.7	37.3	116.5	27.8	67.8	3.8	
20 Dec 68	17 14 45.1	37.3	116.5	14.0	37.6	3.8	
20 Dec 68	01 28 08.2	37.3	116.4	13.7	--	3.9	N
20 Dec 68	17 33 07.5	37.3	116.5	7.0	--	3.8	N
20 Dec 68	20 08 20.4	37.2	116.5	78.5	60.1	4.2	
20 Dec 68	23 59 17.1	37.2	116.5	12.7	--	3.9	N
21 Dec 68	03 38 42.2	37.3	116.5	4.5	9.9	3.6	C
21 Dec 68	15 04 59.5	37.3	116.5	56.4	7.6	4.0	
21 Dec 68	15 45 18.8	37.2	116.5	26.8	9.9	3.9	
21 Dec 68	17 43 14.3	37.3	116.3	11.3	15.8	3.4	
21 Dec 68	19 07 34.1	37.3	116.5	28.2	16.0	4.1	
22 Dec 68	03 51 54.7	37.2	116.5	4.2	20.4	3.1	
22 Dec 68	09 59 54.7	37.4	116.3	53.2	98.6	4.2	
22 Dec 68	18 10 53.1	37.2	116.5	197.0	1236.1	4.2	
22 Dec 68	23 28 29.1	37.3	116.4	5.4	23.7	3.9	
23 Dec 68	05 44 02.9	37.2	116.5	11.0	24.6	3.9	C
23 Dec 68	05 56 03.7	37.3	116.5	15.1	15.5	3.8	
23 Dec 68	09 25 30.1	37.3	116.5	11.0	30.5	3.9	
26 Dec 68	03 15 46.1	37.3	116.5	2.4	--	3.9	N
06 Jan 69	06 34 14.5	37.3	116.5	676.0	3956.0	4.6	
08 Jan 69	11 46 51.9	37.3	116.5	9.6	3.9	3.9	
08 Jan 69	20 44 57.4	37.3	116.5	21.4	36.0	4.0	
08 Jan 69	21 06 22.4	37.2	116.6	22.2	40.3	3.9	
09 Jan 69	00 13 18.0	37.2	116.5	1.3	16.6	4.1	
09 Jan 69	06 22 36.0	37.3	116.4	3.9	13.1	3.9	
10 Jan 69	09 41 21.5	37.2	116.5	53.3	798.9	4.4	
10 Jan 69	17 01 44.5	37.2	116.5	21.3	189.8	4.4	C
10 Jan 69	17 14 17.2	37.2	116.5	63.8	116.8	4.3	C

C = Common

N = No Rayleigh Wave

TABLE IIIB

Earthquake List for KN-UT

Date	Origin	North Latitude(°)	West Longitude(°)	O-P P	O-P LR	NOS m_b	Comment
21 Dec 63	03 02 23.0	39.3	114.3	6.0	--	3.3	N
28 Dec 63	14 26 19.6	39.2	114.2	8.2	--	3.5	N
28 Dec 63	15 50 14.2	39.1	114.1	6.1	--	3.3	N
29 Dec 63	04 06 12.2	39.1	114.2	5.5	142.1	3.4	
29 Dec 63	04 15 03.8	39.1	114.3	45.5	55.1	4.0	
29 Dec 63	06 38 58.2	39.1	114.2	2.9	35.1	3.7	
07 Jan 64	11 55 34.2	39.2	114.2	23.2	63.2	3.6	
07 Jan 64	12 53 47.8	39.1	114.2	16.9	63.2	3.5	
21 Jan 64	23 31 42.3	39.2	114.2	25.	106.6	3.9	
05 Mar 64	12 40 52.8	39.2	114.2	7.5	55.9	3.4	
12 Aug 64	05 04 50.9	39.4	112.0	7.0	30.3	3.9	C w/UBO
21 Aug 64	22 03 51.6	37.0	115.1	7.3	--	3.8	N
03 May 65	03 30 50.1	36.0	114.7	30.6	93.4	3.9	
05 Jul 65	17 17 07.2	39.3	111.5	1.9	22.0	3.2	
17 Nov 65	09 41 28.3	37.6	115.2	10.1	171.1	3.7	
06 Apr 66	17 56 31.7	37.3	115.4	21.1	15.0	4.3	
11 Dec 67	02 35 21.1	37.2	115.2	10.7	--	3.3	N
11 Mar 68	07 34 24.2	37.0	115.5	9.5	22.4	3.6	
26 Apr 68	15 32 21.0	37.2	116.5	245.0	2050.0	4.9	C w/MN-NV
28 Apr 68	04 23 40.0	37.2	116.5	42.1	66.1	4.0	C
28 Apr 68	16 35 17.0	37.2	116.5	31.0	40.5	3.7	
30 Apr 68	07 49 03.0	37.3	116.3	101.7	72.2	4.2	C
04 Aug 68	06 23 36.4	39.1	111.4	5.5	23.2	4.0	
19 Dec 68	19 18 19.6	37.3	116.4	159.9	36.2	4.1	C
19 Dec 68	19 54 01.2	37.2	116.5	53.3	207.0	4.3	C
19 Dec 68	22 23 26.3	37.2	116.5	324.0	1098.0	5.0	C
21 Dec 68	03 38 42.2	37.3	116.5	4.6	6.0	3.6	C
23 Dec 68	05 44 02.9	37.2	116.5	6.7	43.3	3.9	C
10 Jan 69	17 01 44.5	37.2	116.5	19.3	103.0	4.4	C
10 Jan 69	17 14 17.2	37.2	116.5	24.3	264.0	4.3	C

C = Common

N = No Rayleigh Wave

TABLE IIIC

Earthquake List for UBO

Date	Origin	North Latitude(°)	West Longitude(°)	Adjusted m_b	M_s^L	NOS m_b	Comments
25 Feb 63	18 45 15.1	42.8	109.0	2.11	2.63	4.3	
09 Jul 63	15 20 46.0	39.8	111.8	1.85	--	3.6	N
14 Aug 63	12 30 06.0	41.5	112.2	3.19	2.71	3.7	
16 Aug 63	03 21 08.7	39.7	112.1	3.68	2.73	3.4	
16 Aug 63	07 01 03.7	41.5	112.2	2.56	--	3.6	N
17 Aug 63	05 09 11.1	41.4	112.2	2.90	--	3.5	N
24 Aug 63	03 15 49.8	40.8	112.0	2.51	--	3.5	N
28 Aug 63	00 13 12.9	40.9	111.9	2.11	--	3.4	N
30 Sep 63	09 17 42.2	38.0	111.0	3.03	3.80	4.5	
04 Aug 64	11 13 25.0	39.7	106.0	2.30	2.77	4.0	
12 Aug 64	05 04 50.9	39.4	112.0	2.07	2.40	3.9	C w/KN-UI
16 Feb 65	20 17 54.0	39.9	105.1	2.35	--	4.6	N
16 Feb 65	22 21 44.0	39.9	105.0	2.25	3.26	4.9	
11 May 65	01 50 25.0	41.0	111.5	2.71	--	4.1	N
30 May 65	17 31 04.0	39.4	106.3	3.27	3.12	4.3	
18 Jul 65	21 40 45.0	39.6	104.9	3.05	--	4.6	N
29 Jul 65	08 25 53.0	43.2	111.8	2.43	2.67	4.0	
31 Jul 65	13 41 43.0	39.7	104.9	2.70	2.56	4.6	
29 Sep 65	18 59 56.0	39.8	105.1	3.42	3.50	4.7	
29 Sep 65	19 20 41.0	39.7	104.9	2.94	2.84	4.6	
29 Sep 65	23 22 58.0	39.7	104.9	3.17	--	4.6	N
24 Dec 65	10 05 04.5	42.7	110.7	2.13	--	3.9	N
11 Feb 66	20 36 25.9	42.1	111.4	2.46	2.73	3.3	
12 Feb 66	09 52 39.0	42.3	111.2	1.75	2.33	3.2	
03 Apr 66	16 21 33.5	39.3	106.4	3.23	2.79	4.6	
19 May 66	00 26 44.0	37.0	107.2	3.23	2.58	4.6	
02 Jun 66	21 59 12.0	36.9	107.0	3.27	2.41	5.0	
11 Jun 66	10 19 27.0	43.1	111.1	2.36	--	3.4	N
21 Oct 66	07 13 52.0	38.2	113.1	3.32	3.28	4.9	
14 Nov 66	20 02 35.8	39.9	104.7	3.42	2.95	4.1	
16 Jan 67	09 22 45.7	37.7	107.8	3.21	2.81	4.1	
03 Feb 67	05 27 58.0	39.7	104.8	3.12	2.86	4.3	
10 Mar 67	02 20 35.4	42.0	110.2	2.13	--	4.1	N
04 Apr 67	22 53 39.6	38.3	107.7	2.11	2.81	4.5	
27 Apr 67	17 24 41.7	39.9	104.7	3.63	3.15	4.4	
09 Aug 67	13 25 06.2	39.9	104.7	3.86	4.32	5.3	
24 Sep 67	05 00 28.0	40.7	112.1	2.64	2.60	3.7	
27 Nov 67	05 09 22.7	40.0	104.7	3.58	3.73	5.2	
27 Nov 67	05 35 00.7	39.9	104.7	3.61	3.40	4.4	
09 Jan 68	02 16 39.3	42.7	106.8	3.68	2.95	3.8	
16 Jan 68	08 58 44.0	39.3	112.1	2.69	2.73	4.1	
16 Jan 68	09 17 52.3	39.3	112.1	1.94	2.54	3.9	
16 Jan 68	09 42 54.2	39.2	112.0	2.84	3.16	4.0	
17 Jan 68	04 27 16.1	39.3	112.2	2.67	2.50	2.8	
20 Mar 68	15 33 07.0	37.8	112.3	2.34	--	3.9	N
16 Nov 68	03 51 22.4	43.7	110.2	2.89	2.88	3.9	
23 May 69	05 24 53.6	39.0	111.9	2.55	--	4.0	N
18 Jun 69	04 26 37.7	38.7	112.7	2.00	--	4.1	N
30 Jun 69	12 05 52.3	42.7	111.2	2.23	2.83	3.7	
27 Aug 69	15 59 28.4	42.9	110.8	2.67	2.86	4.2	
19 Sep 69	09 31 45.9	43.1	111.4	3.05	2.92	4.1	
19 Sep 69	13 33 15.0	43.0	111.4	2.66	3.47	4.5	
19 Sep 69	19 57 18.7	43.0	111.3	2.25	3.05	4.3	
19 Sep 69	23 58 06.5	43.0	111.5	2.51	--	3.9	N
20 Sep 69	09 12 06.7	43.1	111.4	2.30	--	3.6	N
23 Sep 69	12 58 13.5	42.9	111.5	2.71	2.75	3.9	

C = Common

N = No Rayleigh Wave

TABLE IV

Magnitudes of Other Western United States Explosions and Earthquakes

Name	Date	Time(z)	Latitude	Longitude	Depth	Location	Adjusted m_b	n	Adjusted M_s	n
GASBUGGY	10 Dec 67	1930:00.1	36.7N	107.2W	1.3km	New Mexico	4.56	26	4.19	21
RULISON	28 Aug 70	2100:00.1	39.4N	107.9W	2.6km	Colorado	4.59	27	4.09	26
Colorado Earthquake	09 Aug 67	1325:06.2	39.9N	104.7W	5km	Colorado	4.42	26	4.68	22
New Mexico Earthquake	23 Jan 66	0156:38.0	37.0N	106.9W	10km	New Mexico	4.77	28	4.82	25
Cache Creek Earthquake	30 Aug 62	1335:28.7	41.8N	111.8W	37km	Utah	5.00	30	5.62	14
Cache Creek Aftershock	05 Sep 62	1604:29.0	40.7N	112.0W	14km	Utah	4.12	24	4.20	31

TABLE V

$\overline{M}_s - M_s^T$

Explosions

Event	M_s or $\overline{M}_s$	m	M_s^T	$M_s - M_s^T$	Event Companion	M_s	M_s	M_s^T	$M_s - M_s^T$
DeMoines	4.10	1	3.31	+0.79	Mississippi	4.02	3.90	4.15	-0.25
Fisher	3.21	1	2.06	+1.15		4.02	4.29	4.15	+0.14
Madison	4.78	3	3.31	+1.47		4.02	3.99	4.15	-0.16
Mink	2.67	1	2.30	+0.37		4.02	3.94	4.15	-0.21
Pampas	3.54	2	3.15	+0.39	No Companion Event				
Red Hot	3.05	1	2.87	+0.18	Mississippi	4.02	4.04	4.15	-0.11
Stutz	2.87	3	3.58	-0.71	Fore	4.11	4.18	4.25	-0.07

Earthquakes

S. Nevada Earthquakes	M_s or $\overline{M}_s$	n	M_s^T	$(M_s - M_s^T)$	Companion Eartnquake	M_s	$\overline{M}_s$	M_s^T	$(\overline{M}_s - M_s^T)$
17 Aug 66, 02:37:02.0	2.22	1	2.08	+0.14	S. Nevada	4.01	3.33	3.88	-0.55
17 Aug 66, 04:46:41.2	2.87	3	2.69	+0.18	10:51:38.5	4.01	3.80	3.88	-0.08
17 Aug 66, 11:19:06.0	2.91	1	2.44	+0.47	10:51:38.5	4.01	4.03	3.88	+0.15
18 Aug 66, 06:27:44.0	2.13	2	2.84	-0.71		4.01	3.68	3.88	-0.30
18 Aug 66, 08:03:37.0	2.08	1	2.33	-0.25		4.01	3.33	3.88	-0.55
18 Aug 66, 10:09:22.6	3.00	3	3.01	-0.01		4.01	3.81	3.88	-0.07
18 Aug 66, 20:09:16.0	2.52	2	2.81	-0.29		4.01	3.68	3.88	-0.20

Unclassified

Security Classification

DOCUMENT CONTROL DATA - R&D

(Security classification of title, body of abstract and indexing annotation must be entered when the overall report is classified)

1. ORIGINATING ACTIVITY (Corporate author)
Teledyne Geotech
Alexandria, Virginia

2a. REPORT SECURITY CLASSIFICATION
Unclassified

2b GROUP

3 REPORT TITLE
RELATIONSHIP OF BODY AND SURFACE WAVE MAGNITUDES FOR SMALL EARTHQUAKES AND EXPLOSIONS

4. DESCRIPTIVE NOTES (Type of report and inclusive dates)
Scientific

5. AUTHOR(S) (Last name, first name, initial)
Lambert, D.G.; Alexander, S.S.

6. REPORT DATE	7a. TOTAL NO. OF PAGES	7b. NO. OF REFS
12 August 1971	66	8

8a. CONTRACT OR GRANT NO.	9a. ORIGINATOR'S REPORT NUMBER(S)
F33657-72-C-0009 b. PROJECT NO. VELA T/2706 ARPA Order No.: 1714 cARPA Program Code No. 2F-10	245 9b. OTHER REPORT NO(S) (Any other numbers that may be assigned this report)

10 AVAILABILITY/LIMITATION NOTICES

APPROVED FOR PUBLIC RELEASE: DISTRIBUTION UNLIMITED

11. SUPPLEMENTARY NOTES	12. SPONSORING MILITARY ACTIVITY
	Advanced Research Projects Agency Nuclear Monitoring Research Office Washington, D.C.

13 ABSTRACT

The relationship between body wave magnitude (m_b) and surface wave magnitude (M_s) is investigated using LRSM and VELA Observatory recordings of explosions at NTS, and small shallow earthquakes originating in Nevada, Alaska and central United States. Average M_s vs m_b curves based on data from many observing stations, as well as M_s vs m_b comparisons for individual stations are given. The estimates of m_b and M_s were corrected for stations at small epicentral distances using Evernden's and von Seggern's methods, respectively, in order not to bias the results when only close in or regional observations could be made.

Despite considerable scatter in individual M_s vs m_b determinations the results obtained for earthquakes show that on the average the relative excitation of P waves and Rayleigh waves is similar for the three source regions considered.

Least squares regression lines were fit separately to the observations of M_s vs m_b for NTS explosions and to those for small, shallow Nevada and Missouri earthquakes down to M_s = 2.6. The resulting slopes were very similar (1.04 ± .05 for explosions and 1.00 ± 0.10 for earthquakes) but the intercepts differed such that for given m_b the average M_s for NTS explosions is 0.62 to 0.65 smaller than for the earthquakes. For new events drawn from the same population the M_s vs m_b criterion can be expected to classify correctly 87.7% of NTS explosions and 72.8% of Nevada earthquakes for which any Rayleigh wave measurement can be made; however, several correctly discriminated events would fall sufficiently close to the best discriminant line that further analysis of them would be needed before a convincing classification could be made. If one considers a restricted data set consisting of a swarm of southeast Nevada earthquakes in April 1966 and of contained NTS underground explosions, then for new events from the same population recorded at four or more stations with $3.6<m_b\leq5.04$ for explosions and $2.6<m_b<4.2$ for earthquakes, ($2.77<M_s<4.33$), it can be expected that 98.7% of the explosions and 99.0% of the earthquakes will be correctly classified. But again, in a practical sense no decision could be made for some additional percentage of events.

These data are from regional and close in stations, and it is not certain that the conclusions can be extrapolated for these low magnitudes to future teleseismic measurements made with new instruments and arrays. If a discriminant of this power is relied upon in a seismic region where there are several hundred earthquakes per year, then there will be several false alarms per year.

14 KEY WORDS

Identification
M_s versus m_b
Body wave magnitude (m_b)
Rayleigh wave magnitude (M_s)

Unclassified

Security Classification